Transcutaneous Measurement of Volume Blood Flow

by

R. E. Daigle F. D. McLeod

C. W. Miller M. B. Histand M. K. Wells

from the Departments of

Physiology and Biophysics, and Mechanical Engineering

Colorado State University

A Technical Report Prepared

for the National Aeronautics and Space Administration

Ames Research Center

under NASA Grant NSG - 2009

August 1, 1974

Contents

I. Introduction

1. Ultrasonic measurements

A significant barrier to the acquiring of physiological information on cardiovascular function through nontraumatic techniques is the human skin. A much sought after parameter which has been the object of numerous measurement techniques is volume blood flow. A critical evaluation of the methods currently available for blood flow measurement indicates that among the most promising in terms of accuracy and reliability are those employing ultrasonic energy (Rushmer, Baker and Stegall, 1966).

Ultrasound has several distinct advantages over other energy sources when used in biological applications. It is conveniently generated from electrical impulses using piezoelectric crystal materials, such as lead-titanate-zirconate. It can be easily transmitted into and through the fluid medium of the body. In addition, it can be used to provide dimensional information on internal structures as well as providing velocity information on moving interfaces.

The ability to measure blood velocity using ultrasound is derived from the Doppler effect - the change in frequency which occurs when sound is reflected or transmitted from a moving target. When ultrasound of the appropriate frequency is transmitted through a moving blood stream, the blood cells act as point scatterers of ultrasonic energy. If this scattered ultrasonic energy is detected, it is found to be shifted in frequency according to the velocity of the blood cells, v, the frequency of the incident sound, f_o, the speed of sound in the medium, c, and the angle between the sound beam and the velocity vector, σ. The relation describing this effect is known as the Doppler equation.

$$\Delta f = \frac{2 f_o \, v \cos \sigma}{c} \qquad 1.1$$

2. Continuous Wave Doppler flowmeters

Satomura (1960) was one of the first to employ ultrasonic Doppler shift

detection for blood flow measurements and numerous investigators have followed suit. The majority of instruments available for this purpose employ continuous wave (CW) ultrasound transmitted from one piezoelectric transducer and received by another. Generally, the entire vessel is illuminated with ultrasonic energy and the Doppler shifts from many blood cells moving at various velocities combine to produce a Doppler shift spectrum. The first moment of this Doppler shift spectrum is related to the average blood velocity over the region illuminated. The first moment is generally approximated through zero crossing detection, which provides an output proportional to the average number of zero crossings of the Doppler shift signal. While this frequency to voltage conversion technique is subject to error, especially for broadband Doppler shift signals, it provides a simple and direct means of obtaining a blood velocity estimate.

3. The Pulsed Ultrasound Doppler Velocity Meter

In recent years, instruments have been developed which are capable of specifying the range or depth of the blood velocity measurement. Such instruments employ pulsed ultrasound and are known as pulsed ultrasound Doppler velocity meters (PUDVM). Their development has been undertaken by McLeod (1971), Baker (1970), Peronneau (1970), and Wells (1969). The PUDVM emits short burst of ultrasound (~ 1μsec) at a fixed repetition interval from a piezoelectric transducer. During the period between emission, the same transducer acts as a receiver of backscattered ultrasound, thus eliminating the need for a separate receiving crystal. The time delay from emission to reception of the scattered energy is related to the distance of the scatterers from the transducer. By gating the receiver on for a short interval of time (~.5μsec) at the appropriate delay interval, the PUDVM is able to process Doppler shift information from a limited volume, known as the sample region. This volume can be scanned across a blood

vessel to measure what is known as a velocity profile. More recent instruments employ multiple receiver gates to allow instantaneous velocity profile measurement.

The critical aspect of PUDVM measurements is resolution. Axial resolution can be defined as the ability to distinguish separately two adjacent moving thin sheets of flow oriented at a given Doppler angle to the sound beam. Radial resolution is a function of the ultrasonic beam width. Many factors affect the resolution of the PUDVM and its ability to accurately measure velocity profiles. These will be discussed at length in the sections to follow.

4. Volume flow measurements

Ultrasonic blood flowmeters employing the Doppler shift effect are actually velocity meters, since the measured parameter is blood velocity. Consequently, blood flow obtained through ultrasonic techniques is always a calculated quantity rather than a measured quantity. Since several methods of obtaining blood velocity information are available, there are several different methods of computing volume blood flow. The purpose of this study is to assess the various techniques for obtaining ultrasonic blood flow information in subcutaneous arteries. A secondary goal is to develop an optimal measurement procedure for volume blood flow based on the results of the above assessment.

Volume flow, V, is defined as the mean velocity, $\bar{v}$, over the entire cross-sectional area of the vessel lumen, times this area, A.

$$V = \bar{v} \cdot A \qquad 1.2$$

If the velocity distribution over the cross-section of the vessel is known, volume flow can be written as an integral.

$$V = \int_A v_{(a)}\, dA \qquad 1.3$$

where $v_{(a)}$ is the velocity at a point on the vessel cross-section.

Unfortunately, in the case of ultrasonic blood velocity measurements, not all of the above parameters may be known. For CW ultrasound measurements, if the vessel is uniformly illuminated, the first moment of the Doppler shift power spectrum corresponds to $\bar{v}$. The cross-sectional area, however, is not obtainable using CW techniques. With the PUDVM, a thin ultrasound beam through the center of the vessel can provide a measure of the diameter, thus allowing approximation of A, but the velocity distribution is then only known across this beam path. Therefore, CW ultrasound measurements require some independent measure of vessel geometry, while PUDVM measurements require some assumptions concerning the velocity distribution over the area of the vessel cross-section not measured.

Three basic techniques for obtaining volume flow from ultrasonic velocity measurements will be discussed. All three are for implementation using a PUDVM with a variable receiver gate, allowing adjustment of the axial length of the sample volume. The first method employs uniform illumination of the vessel cross-section similar to a CW ultrasonic technique. An independent measure of the vessel diameter must also be obtained. The second method uses the PUDVM in the traditional manner to record blood velocity profiles which are then integrated to obtain volume flow. The third technique is a hybrid of the first and second and uses the PUDVM to measure the average velocity across a vessel along a narrow sound beam, thus eliminating the need for profile measurement. All three of these techniques can be carried out with single element transducers, with the ultrasound applied transcutaneously to determine volume flow in underlying vessels.

II. Volume Flow Measurement Techniques

1. Uniform Illumination Method

This technique involves separate determination of the mean blood velocity over the vessel lumen and vessel diameter. The determination of mean velocity is accomplished by exposing the entire vessel cross-section to a uniform intensity sound field and then obtaining the first moment of the Doppler shift signal spectrum. The vessel diameter may be obtained by Doppler shift or echo imaging or by Doppler shift power scanning, to be discussed in later sections.

Errors in applying the uniform illumination method are both experimental and systematic. Experimental errors are mostly due to improper selection and positioning of the ultrasonic transducer. To provide a uniform intensity sound field, the transducer must have a larger beam cross-sectional area than the vessel. However, the beam area must not be so large as to include other adjacent blood vessels in its radiation field. The sample region of the PUDVM is set to include the entire vessel lumen by adjusting the time span on the receiver gate. This adjustment excludes unwanted signals from other vessels lying in the sound beam path. Since the sample region of the PUDVM is made somewhat larger than the vessel cross-section, lateral and axial positioning errors are usually insignificant. The most important source of error due to probe positioning is the setting of the Doppler angle. Techniques for obtaining accurate Doppler angle settings will be discussed in later sections.

Systematic errors are primarily due to signal processing and resolution. The typical method of converting the Doppler frequency shift signal into a voltage proportional to mean velocity is through zero-crossing detection. Application of the zero-crossing frequency to voltage converter to Doppler shift signals has been described by Peronneau, (1970) and Flax et al. (1971). The technique is

used primarily for its simplicity and ease of implementation.

The mean zero-crossing rate of the Doppler signal is given by the relationship (Rice, 1944; Bachman, 1966)

$$f_m^2 = \frac{\int f^2 P(f)df}{\int P(f)df} \qquad 2.1$$

where f_m is the second moment or radius of gyration about the origin, f is the Doppler frequency and P(f) is the power. The mean velocity in the sample region, however, is given by the first moment of the power spectrum, f_d. For narrow-band signals, as normally encountered when dealing with small sample regions with the PUDVM, the error introduced by taking the zero crosser output as an estimate of f_d is negligible. In the case of uniform vessel illumination, however, the Doppler shift spectrum can be quite wide and significant errors may result.

The error introduced, $\Delta f = f_m - f_d$, depends on the width and shape of the power spectrum, which in turn depends on the velocity distribution across the vessel. Typical symmetrical velocity distributions can be approximated by the equation

$$v(r) = 1 - r^n \quad (0 \leq r \leq 1) \qquad 2.2$$

where r is the distance radially from the vessel axis. For n = 2 this equation gives a parabolic flow field, and increasing n values lead to increasingly blunt flow profiles. The peak velocity and vessel radius are normalized to unity. The average velocity over the entire vessel lumen can be found by integrating equation 2.2 over the region r = 0 to r = 1.

$$\rightarrow \quad \bar{v} = \frac{\int_0^1 (1-r^n) \cdot 2\pi r dr}{\pi r^2}$$

$$\bar{v} = 2\left[\frac{r^2}{2} - \frac{r^{n+2}}{n+2}\right]_0^1$$

$$\bar{v} = \frac{n}{n+2} \qquad 2.3$$

The error in measurement of average velocity using the zero-crossing detector can be found by applying equation 2.1 to this same velocity field. Since velocity is related to Doppler shift frequency by a constant (see equation 1.1) and the power is assumed constant over the field, equation 2.1 can be rewritten as

$$v_m^2 = \int_s v^2(r)dr \qquad 2.4$$

Substituting equation 2.2 for $v(r)$ and integrating to find the average velocity, we obtain

$$\bar{v}_m^2 = 2\int_0^1 (r^{2n} - 2r^n + 1)rdr$$

$$= 2\left[\frac{r^{2n+2}}{2n+2} - \frac{2r^{n+2}}{n+2} + \frac{r^2}{2}\right]_0^1$$

$$\bar{v}_m = \left[\frac{1}{n+1} - \frac{4}{n+2} + 1\right]^{\frac{1}{2}} \qquad 2.5$$

Taken the ratio of $\bar{v}_m$ to $\bar{v}$ we obtain the normalized mean velocity error which corresponds to the error in volume flow, as calculated by equation 1.2.

$$\frac{\bar{v}_m}{\bar{v}} = \frac{n+2}{n}\left(\frac{1}{n+1} - \frac{4}{n+2} + 1\right)^{\frac{1}{2}} \qquad 2.6$$

Equation 2.6 is plotted in Fig. 2-1 for n = 2 to n = 12, which corresponds to the physiological range of blood flow profiles. It can be seen from the figure that even at n = 12, corresponding to a very blunt profile, the volume flow error is approximately 4%. For parabolic flow (n = 2) the error is 15%.

These data demonstrate that zero crossing detection is unsuitable for accurate volume flow measurements using uniform illumination. A more accurate method would be spectral analysis; however, equipment or computer time involved

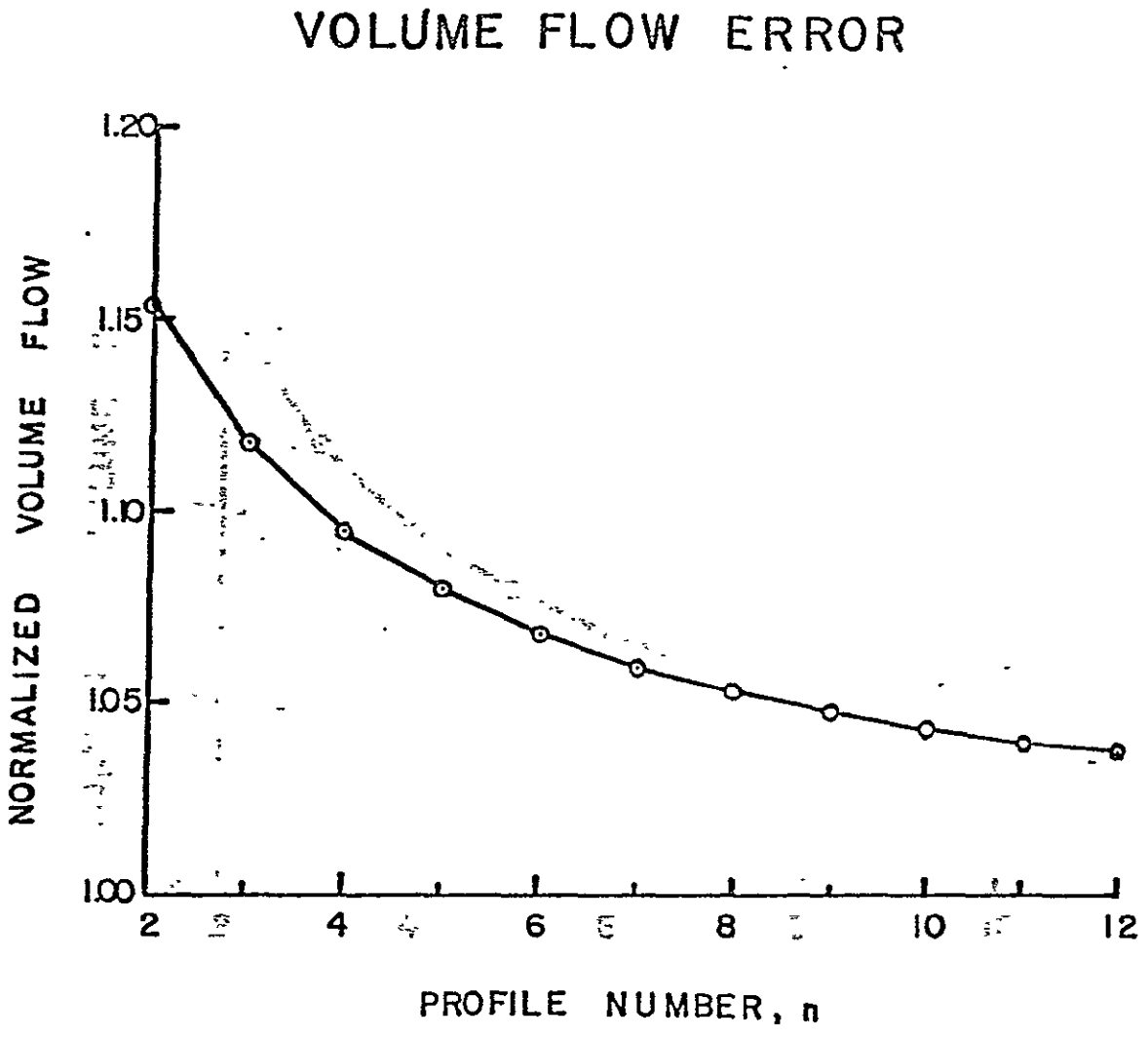

Fig. 2-1 Volume flow error introduced by zero-crossing detection for uniform illumination method.

in spectral analysis procedures can be prohibitably expensive. An alternative to spectral analysis is analog processing of the Doppler shift signal to yield a voltage proportional to the first moment of the Doppler power spectrum. Such a processor is shown in Fig. 2-2.

The directional PUDVM provides two Doppler shift audio outputs. The first is obtained by mixing the returned signal with the emitter frequency while the second is obtained by mixing the returned signal with the emitter frequency shifted 90^0 in phase. The lead-lag relationship of these two signals determines the sign of the Doppler shift frequency, Δf. These signals may be expressed by the following equations.

$$E_a = \int e(w) \sin w\, t\, dw$$

$$E_b = k \int e(w) \cos w\, t\, dw$$

where $e(w)$ and w specify the amplitude and frequency of the Doppler shift spectral component. The factor k is a gain factor relating the two mixer output amplitudes. Differentiating these expressions with time yields:

$$E_a' = \int e(w)\, w \cos w\, t\, dw$$

$$E_b' = -k \int e(w)\, w \sin wt\, dw$$

Multiplying E_a by E_b' and E_b by E_a', we obtain

$$E_1 = -k \int e^2(w)\, w \sin^2 wt\, dw$$

$$E_2 = k \int e^2(w)\, w \cos^2 wt\, dw$$

Taking the sum and difference of E_1 and E_2, we have

$$E_1 + E_2 = k \int e^2(w)\, w\, (\cos^2 wt - \sin^2 wt)\, dw$$

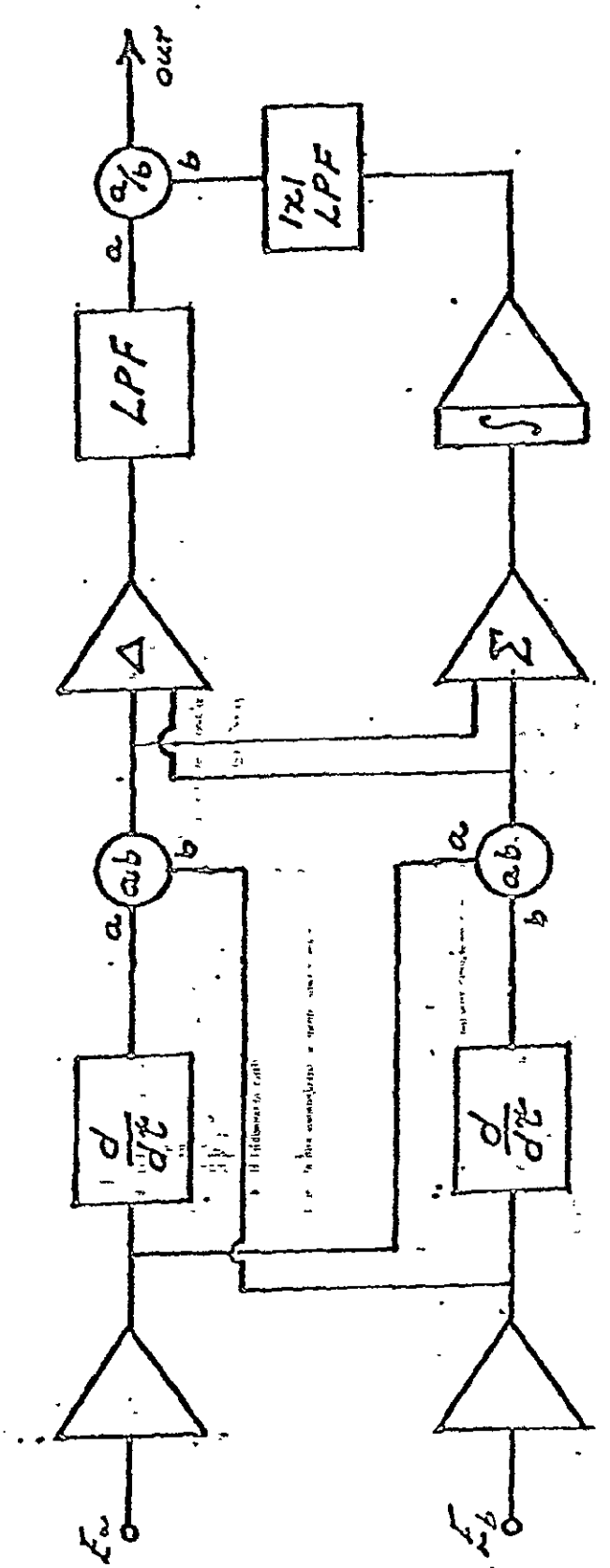

Fig. 2-2 Block diagram of analog processor for obtaining first moment of Doppler shift, power spectrum.

$$= k\int e^2(w)\ w \cos 2\ wt\ dw \qquad 2.7$$

$$E_2 - E_1 = k\int e^2(w)\ w\ (\sin^2 wt + \cos^2 wt)dw$$

$$= k\int e^2(w)\ w\ dw \qquad 2.8$$

Equation 2.8 represents the unnormalized first moment of the power spectrum of the Doppler shift signal. Since the amplitude and consequently the total power of the Doppler signal varies with time, we must normalize equation 2.8 by dividing by the total power. This is obtained by integrating equation 2.7 and eliminating the frequency term by full wave rectification and averaging.

$$\int (E_1 + E_2)dt = \frac{k}{2}\int e^2(w)\ \sin 2\ wt\ dw$$

$$\left|\overline{\int (E_1 + E_2)dt}\right| = \frac{k}{\pi}\int e^2(w)\ dw \qquad 2.9$$

Dividing equation 2.8 by equation 2.9 yields the desired normalized first moment times the constant, π.

$$E_{fm} = \pi \cdot \frac{\int e^2(w)\ w\ dw}{\int e^2(w)\ dw} \qquad 2.10$$

This analog process has been implemented using integrated circuit technology and preliminary tests have produced favorable results. Comparison with the zero-crossing type of processor is being undertaken in fluid test systems with known flow characteristics. The use of the first moment processor with the uniform illumination technique for determining average velocity should bring about a substantial improvemer in the accuracy of calculated volume flow.

The second source of systematic error in applying the uniform illumination technique derives from resolution errors in determining the geometry of the vessel cross-section. The vessel diameter can be determined in a number of different

ways, including Doppler signal power scanning (to be discussed), echo scanning and velocity profile measurement. Resolution errors associated with this latter method will be discussed in the next section.

Calculating the vessel cross-sectional area from the measured diameter assume a cylindrical vessel shape. This assumption is reasonable for most subcutaneous vessels, however, care must be taken not to distort the vessel geometry by excessive pressure with the ultrasound transducer. Perhaps more significant is the error in diameter measurement, since the cross-sectional area is proportional to the square of this measurement.

$$A = \frac{\pi}{4} d^2$$

Let us assume that the actual diameter differs from the measured diameter by an amount Δd. The error in A is then given by

$$\Delta A = \frac{\pi}{4}(d + \Delta d)^2 - \frac{\pi}{4} d^2$$

$$= \frac{\pi}{4}(2d\Delta d + \Delta d^2)$$

The percent of error is

$$\frac{\Delta A}{A} = \frac{2\Delta d}{d} + \left(\frac{\Delta d}{d}\right)^2 \qquad 2.11$$

The error in calculated volume flow is also given by the above equation and is shown plotted as a function of $\Delta d/d$ in Fig. 2-3. From the figure, we note that for a volume flow error of less than 10%, $\Delta d/d$ must be less than .05. For a 5 mm vessel, this amounts to a resolution of better than .25 mm, which is very demanding on current PUDVM capabilities. These capabilities are discussed in detail in section III.

A list of the various types of errors associated with the uniform illumination

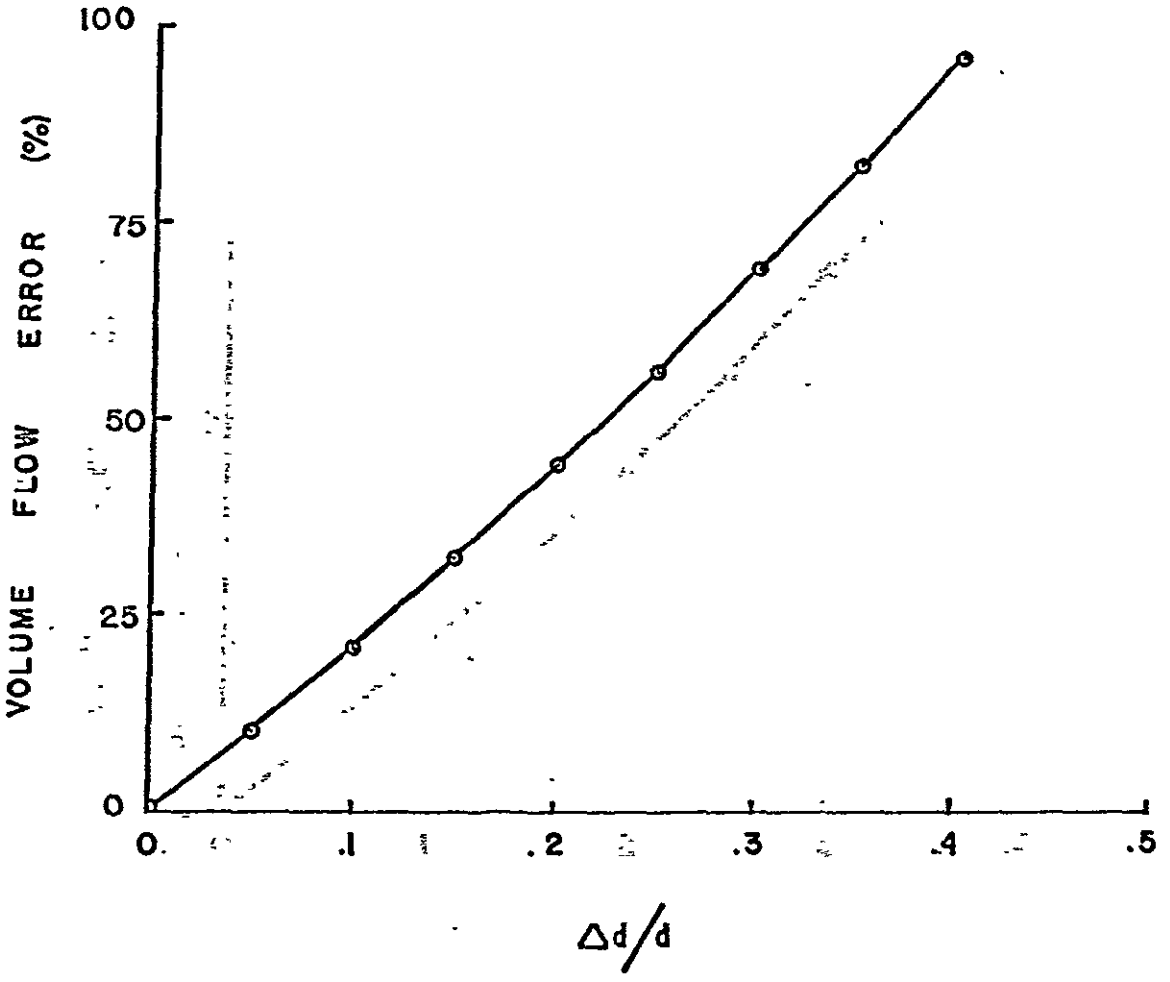

Fig. 2-3 Percent error in volume flow due to error in diameter measurement.

Error Source	Magnitude
Doppler angle errors	$\sim \frac{\cos\sigma}{\cos(\sigma+\Delta\sigma)} - 1$
Zero-crossing detection	see Fig. 2-1
Non-cylindrical vessel	~ distortion in diameter
Diameter measurement error	$\sim \frac{2\Delta d}{d} + (\frac{\Delta d}{d})^2$ (see Fig. 2-3)

Table 2-1. Volume flow errors associated with the uniform illumination method.

technique along with an indication of their magnitude is shown in Table 2-1. While this method of determining volume flow is subject to several sources of error, it has the advantage of being one of the simplest and most direct techniques. Many of the error sources can also be eliminated or reduced with improved technology. The implementation of analog first moment processing can substantially improve the accuracy of the mean velocity determination. Improvements in resolving power of ultrasonic dimensional measurements are continually being made which will reduce the error in measurement of vessel cross-sectional error. Finally, the possibility exists of making real time measurements of a vessel cross-section simultaneously with the mean velocity determination which, with appropriate signal processing, could yield a true ultrasonic volume blood flowmeter.

2. Diameter Profile Integration Method

A second technique for measurement of blood flow involves determination of the blood velocity profile across a diameter of the vessel under study. Since this technique requires measurements of local blood velocity at discrete points across the vessel, the PUDVM is employed. The procedure usually followed with single gate instruments is as follows: The transducer is positioned at a known angle to the vessel and the sample volume located outside the near wall of the vessel. The sample volume is then moved electronically across the vessel in discrete steps, with several heart cycles of blood velocity information recorded at each point. The EKG must be recorded simultaneously so that velocity measurements can be synchronized in time. Generally the quantity of data is such that computer processing of the velocity waveforms is required. The requirement that the Doppler angle be substantially less than 90^{o} prohibits recording a velocity profile across a true diameter; however, for most measurements, the flow profiles can be assumed to be constant over the axial length in question. If a single gate PUDVM is used, the flow characteristics are also assumed to remain constant over the time required

to move the sample volume across the vessel.

Several other assumptions are involved in calculating flow from the measured profile. First of all, the vessel geometry is assumed to be cylindrical over the measurement region. Secondly, the blood velocity field should have a degree of radial symmetry about the vessel axis. More specifically, the measured velocity profile should be valid for rotation about the vessel axis by $\pm 90^0$. Thirdly, the blood velocity vector is assumed to be parallel to the vessel axis at all times during the cardiac cycle, maintaining a constant Doppler angle to the sound beam. These latter two assumptions imply that the profile integration technique is not suitable for highly skewed velocity fields.

If the above conditions are met, the instantaneous volume flow can be found by dividing the vessel cross-section into a series of concentric rings corresponding to the number of measurement locations (see Fig. 2-4). The blood velocity at each location can be written as $v_i(t)$, where i goes from 0 to n, the number of measurement locations. The volume flow is found by weighting each velocity by the area of the half-ring containing the measurement location and performing a summation. The area of the half-rings can be written in terms of the measurement increment, Δx. The center half-circle has an area of

$$\frac{\pi}{2}\left(\frac{\Delta x}{2}\right)^2 = a$$

The area of the first half-ring is 8a, the second 16a, the third 24a, and so on. If we designate the center measurement location as the m^{th} point, then the instantaneous volume flow can be written as

$$V(t) = \sum_{i=0}^{n} 8v_i(t)|m-i|a + v_m(t)a$$

The average flow is found by integrating the above formula over a complete heart cycle, t_h.

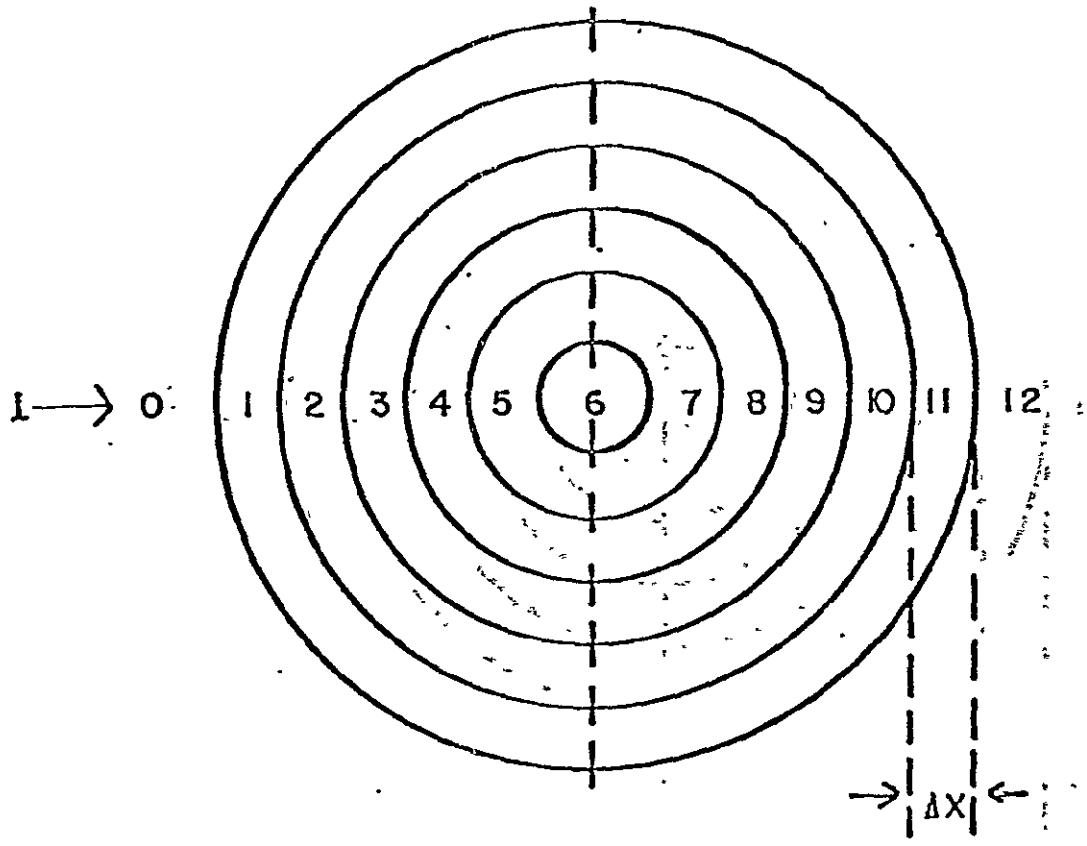

Fig. 2-4 Partioning of vessel cross-sectional for volume flow calculation.

$$\bar{V} = \frac{\int_0^{t_h} [\beta v_i(t) |m-i| a + v_m(t) a] dt}{\int_0^{t_h} dt}$$

While the above calculations may seem quite tedious, they can be performed accurately and quickly on a digital computer, if the velocity waveforms are appropriately digitized.

In addition to the limitations implied in the above mentioned assumptions, use of the diameter profile integration technique is subject to other errors. These errors may be divided into two categories: 1) experimental errors in applying the technique, and 2) resolution errors in the measurement of local velocity and vessel diameter with the PUDVM. The first category involves mostly experimental skill and technique while the second category involves inherent systematic errors.

The first category errors arise from several sources. The transducer employed must have a diameter which is small compared to the diameter of the vessel if the velocity measurements are to be accurate. A large diameter sound beam degrades resolution by increasing the radial projected length of the sample region and introduces errors due to vessel curvature in measurements near the walls. Theoretical and experimental data indicate that errors due to sound beam width are negligible for beam diameters less than ¼ the vessel radius.

A second source of error in the first category is due to misalignment of the sound beam across the vessel. If the sound beam is off the vessel axis, as shown in Fig. 2-5, the calculation of volume flow is affected. This type of error is profile dependent and is at a minimum for a uniform velocity field. Even for this case, however, the error in volume flow calculated goes up as the square of $\Delta r/r$.

$$\% \text{ error in volume flow} = \left(\frac{\Delta r}{r}\right)^2 \times 100$$

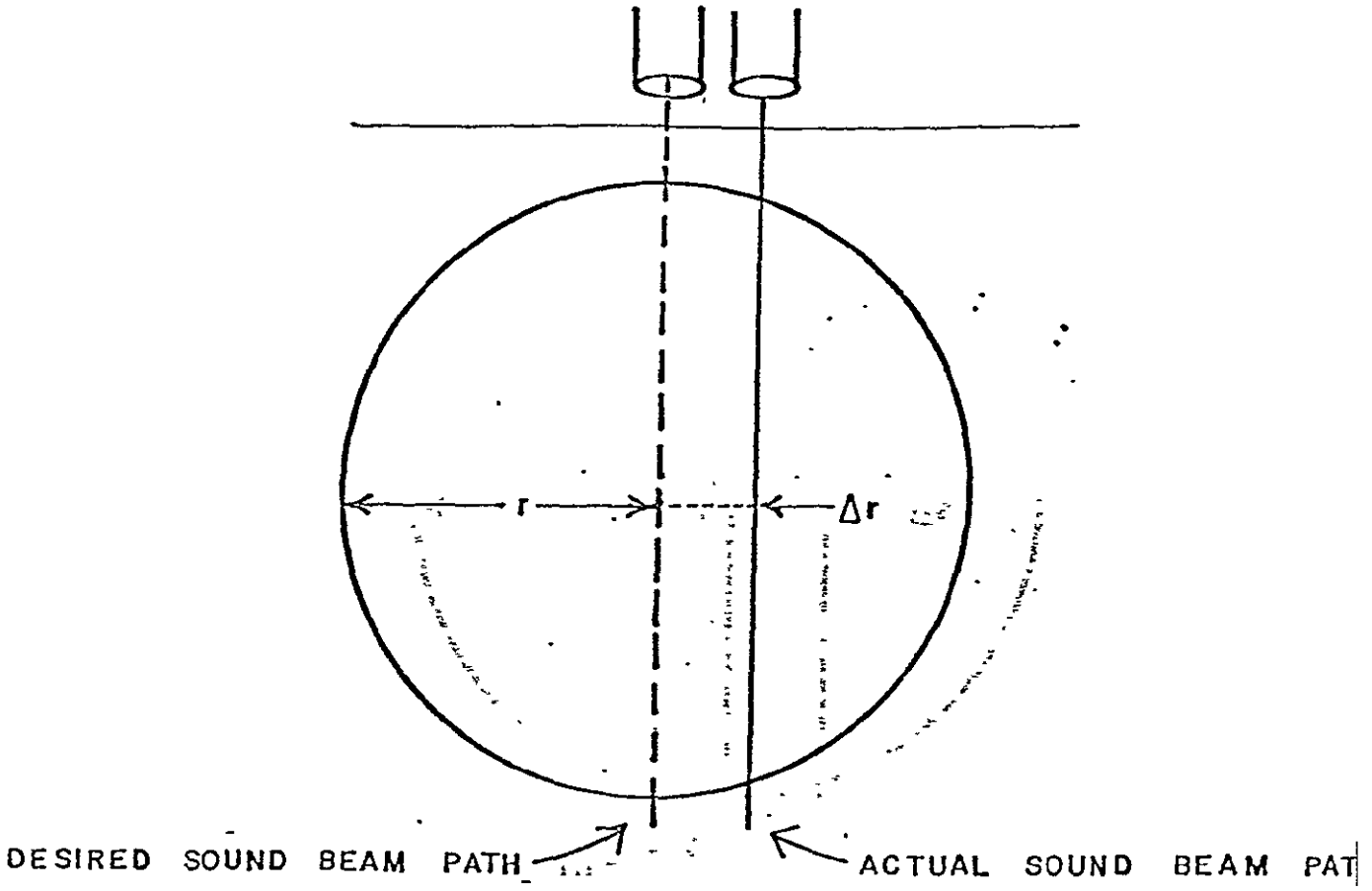

Fig. 2-5 Transducer beam offset introduces error in velocity profile measurement and computed volume flow.

For a parabolic profile, the percent error increases to $2(\frac{\Delta r}{r})^2 \cdot 100$ for small $\frac{\Delta r}{r}$. With these two cases as a bounds on the error, we see that for a misalignment of only $\Delta r = \frac{1}{4}r$, the random error in computed flow lies between 6.25 and 12.5%.

Another source of error involving probe alignment is caused by variation in the Doppler angle. Since the measured blood velocity by the Doppler shift method corresponds to the component of blood velocity in the direction of the sound beam, this measured velocity must be divided by the cosine of the Doppler angle to obtain the actual velocity.

$$V_{actual} = V_{measured} \cdot \frac{1}{\cos\sigma}$$

For a nomimal Doppler angle of 60°, an error of only 3° introduces approximately a 10% error in velocity.

For transcutaneous measurements, the Doppler angle is usually set by two steps. The transducer is first adjusted for a null signal which orients the sound beam at 90° to the vessel axis. The Doppler angle is then set by rotating the transducer through a known angle in a plane which contains the vessel axis. This two step procedure requires a complicated transducer holder for measuring the angles involved and is time consuming. Also, refraction effects as the sound beam enters the tissue can introduce considerable error with this approach.

An alternate approach for obtaining an accurate Doppler angle is to use triangulation techniques. The peak forward blood velocity vector at the vessel centerline can be measured from three independent directions and its orientation computed by triangulation techniques. At peak forward flow this vector can reasonably be assumed to be coincident with the vessel axis. This approach has been successfully employed in transesophageal measurements of aortic blood flow

(Daigle, 1974). Refraction effects remain a source of error with the triangulation method, but if each sound beam is similarly affected, the refraction can be measured and a correction made.

The second category of volume flow measurement errors are those introduced by resolution limitations of the PUDVM. A great many variables influence the size of the measurement volume of the PUDVM, known as the sample region, and these are discussed in detail in section III. The majority of these variables affect the axial length of the sample region, since the radial size of the sample region is fixed primarily by the transducer dimensions. As mentioned previously, for accurate profile measurements, the transducer beam width must be less than ¼ the radius of the vessel. This requirement can be met by choosing the proper size and focus transducer for the vessel under study. The axial length of the sample volume must also be small compared to the vessel radius for accurate velocity profile measurements, but this requirement can not always be satisfied. In practice, the minimum axial length of the sample region is on the order of 1-2 mm. Because of this limitation, it is appropriate to examine the resolution errors introduced in velocity profile measurement and the consequences on calculated volume flow.

The axial length of the sample region is best described by a plot of the beam power along the beam axis as a function of range. Such a plot may be experimentally constructed using a testing apparatus to be described later. The resulting curve is known as the sample function since this function specifies the weighting of blood velocities along the sample region length. The measured blood velocity is approximately the average of the velocities along the sample region length, weighted by the sample function. Because of this property, the measured blood velocity profile when the sample volume is scanned across a blood vessel is described by the convolution of the sample function with the

actual velocity profile. Obviously, the larger the length of the sample function, the greater the distortion of the actual velocity profile due to this convolution effect.

A second type of profile distortion occurs near the walls of a blood vessel (McLeod, 1974). As the sample volume is moved out of the flow stream, part of the sample volume enters a zero velocity region. Since a zero velocity region produces no Doppler shift signal, the PUDVM is unable to respond and the effective size of the sample region is reduced. This effect introduces a boundary error in the velocity profile measurement which gives rise to higher velocities near the vessel walls than expected from simple convolution of the sample function with the actual profile.

For example, consider a rectangular velocity profile and a rectangular sample function, as shown in Fig. 2-6. The convolution of these functions is trapazoidal in shape, as shown. If the boundary error effect is included, however, the profile shape becomes rectangular, with an increase in width equal to the sample function width.

In actual velocity profile measurements, the boundary error effects may be diminished by reduced signal to noise ratios near the walls, and motion of the walls with the pressure pulse. The measured blood velocity profile generally falls somewhere between the convoluted velocity profile and the convoluted velocity profile with boundary error. This region is shown shaded in Fig. 2-6.

To investigate the effects of sample function length on velocity profile measurement, a theoretical study was made using computer generated curves. Velocity profiles were generated according to the formula,

$$y = V_p\,(1-|x^n|) \qquad (-1 \leq x \leq 1)$$

This formula yields a family of curves as shown in Fig. 2-7, with increasing values of n yielding profiles with increasing bluntness. For n = 2, the profile

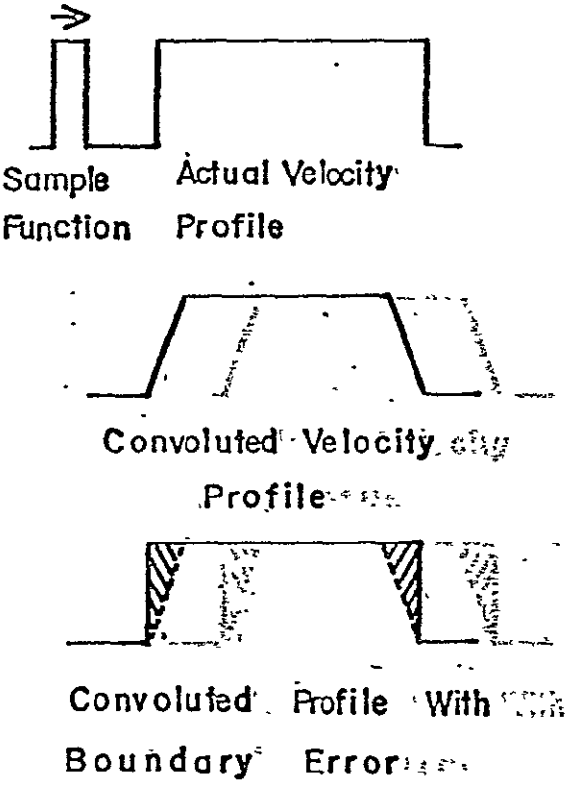

Fig. 2-6 Convolution and boundary error effects on a rectangular velocity profile.

shape is parabolic. These theoretical profiles were convoluted with rectangular sample functions of varying length. Nonlinearities introduced by the zero-crossing detection process were neglected. For long transmission pulse lengths, a rectangular shape is a good approximation to the actual sample function shape, as will be demonstrated in the section on resolution. For shorter pulse lengths, the rectangular shape is still a fair approximation if the width is taken at the half power points of the actual sample function curve. The length of the rectangular sample function is expressed as a fraction of the vessel radius, r.

A second computation was also performed on the theoretical velocity profiles to include the effects of the boundary error. This convolution was carried out by reducing the length of the sample function at the walls to the length of the portion of the sample function within the vessel. These profiles were also calculated for various sample lengths for each n value.

Figures 2-8 through 2-11 show some of the results of these calculations. Each figure shows both the convolution and boundary error effects for various sample function lengths on a velocity profile of order n. For example, Figure 2-5 depicts the results for a parabolic velocity profile of order n = 2. Six sample function lengths are computed from .2r to 1.2r in .2r increments. Note the effect of increasing sample function length on the convoluted profiles. As mentioned previously, the convoluted velocity profile and the convoluted velocity profile with boundary error can be considered as limits on the measured profile, which generally falls between the two extremes.

Next, we must compute the effects of these profile distortions on volume flow calculations. A problem that immediately arises is where to specify the vessel wall locations. If the measured profile is the only data available, some method of wall location based on that profile must be constructed. One such method is to specify the wall location as the point at which the velocity goes

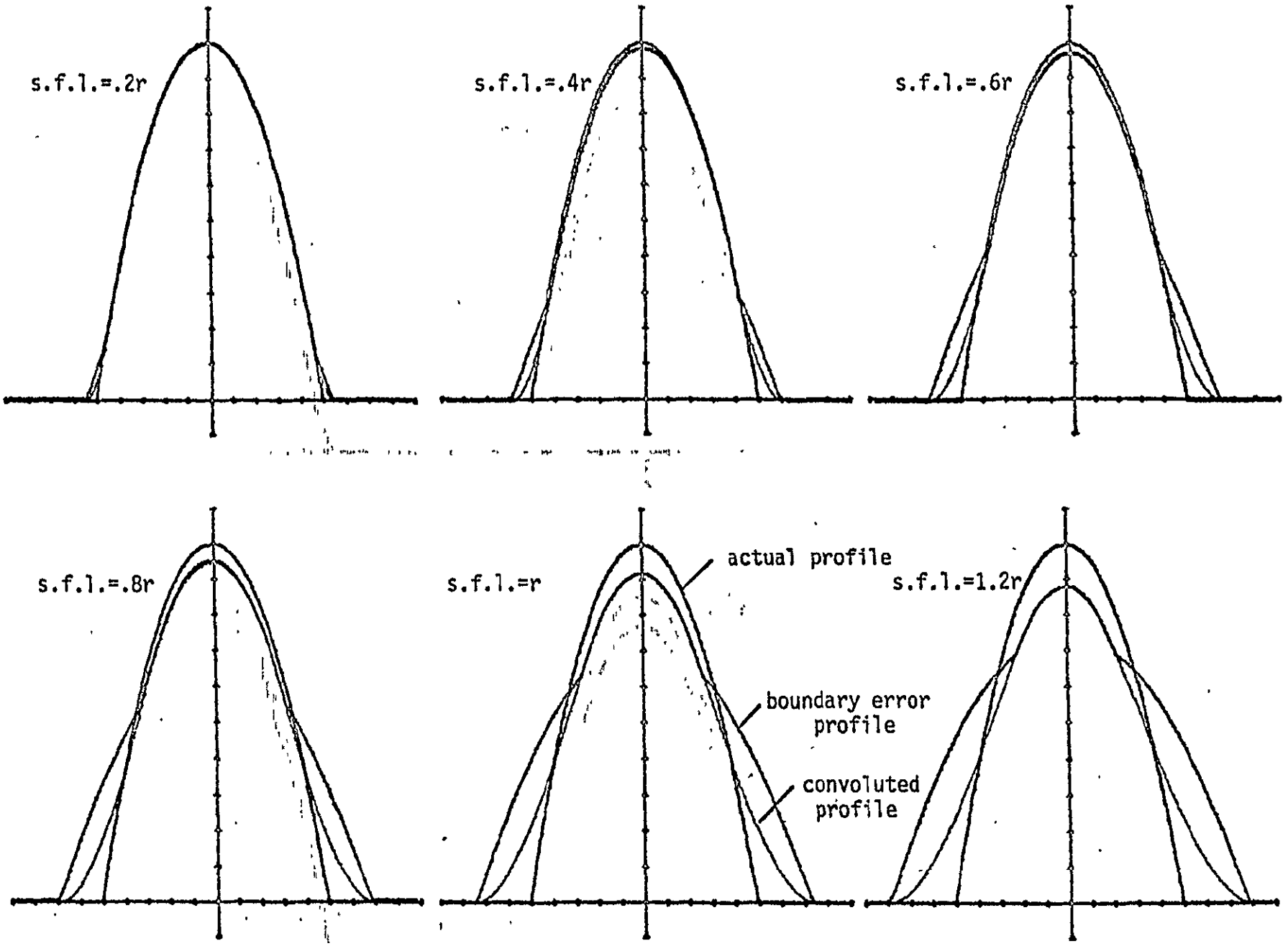

Fig. 2-8 Convolution and boundary error profiles for n=2. The sample function length increases for each successive set of profiles by .2r.

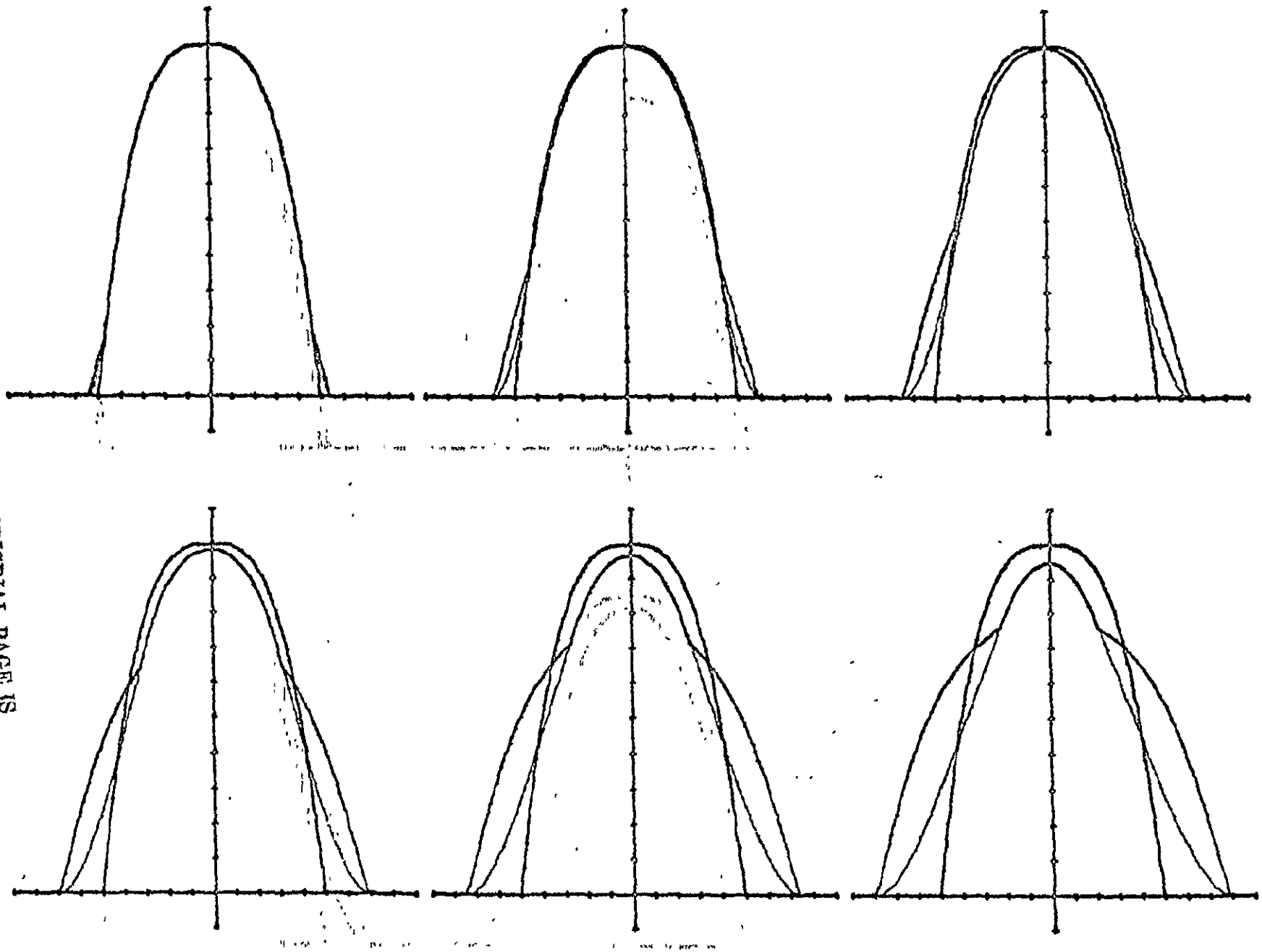

Fig. 2-9 Convolution and boundary error profiles for n=3.

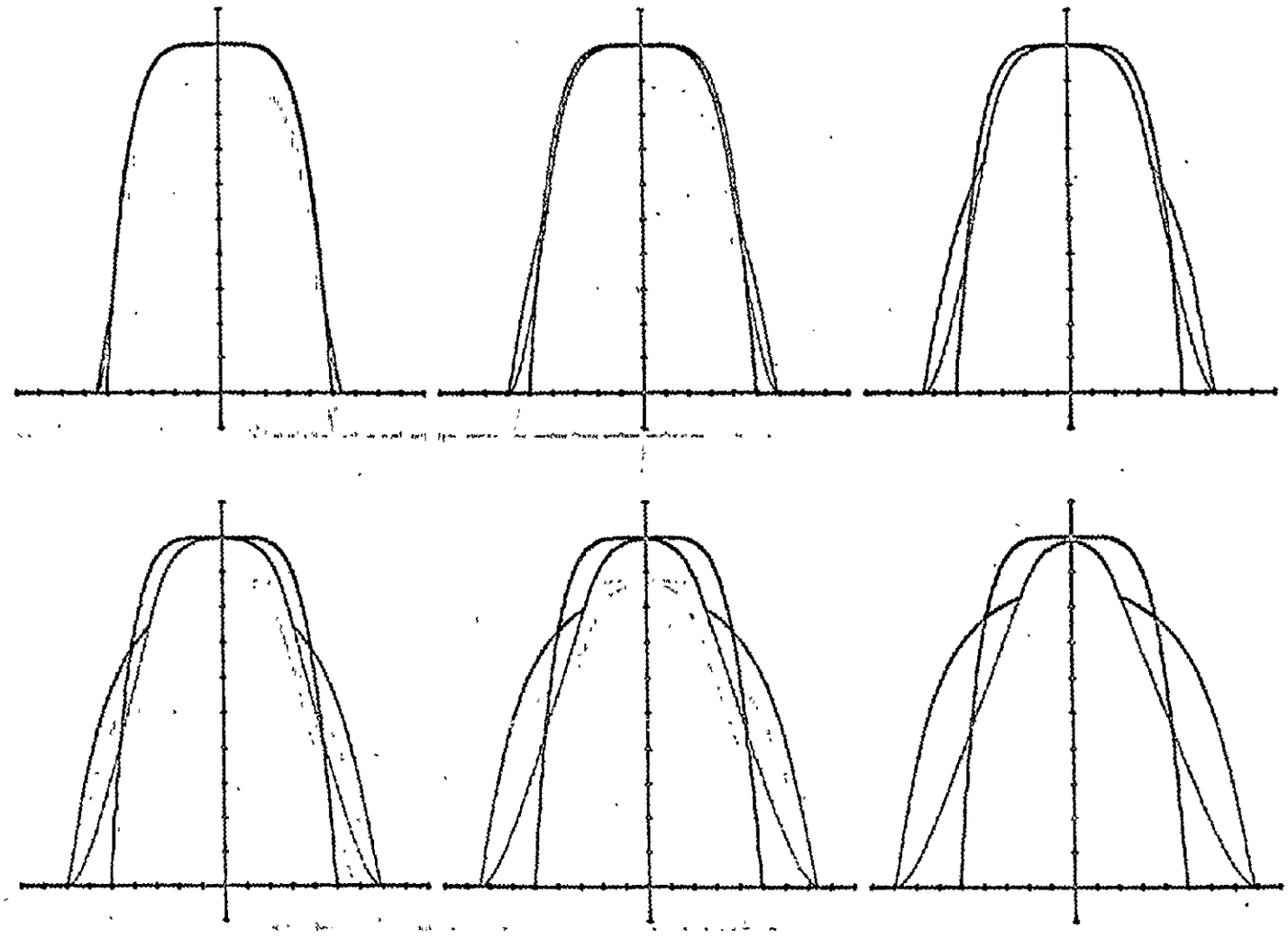

Fig. 2-10 Convolution and boundary error profiles for n=5.

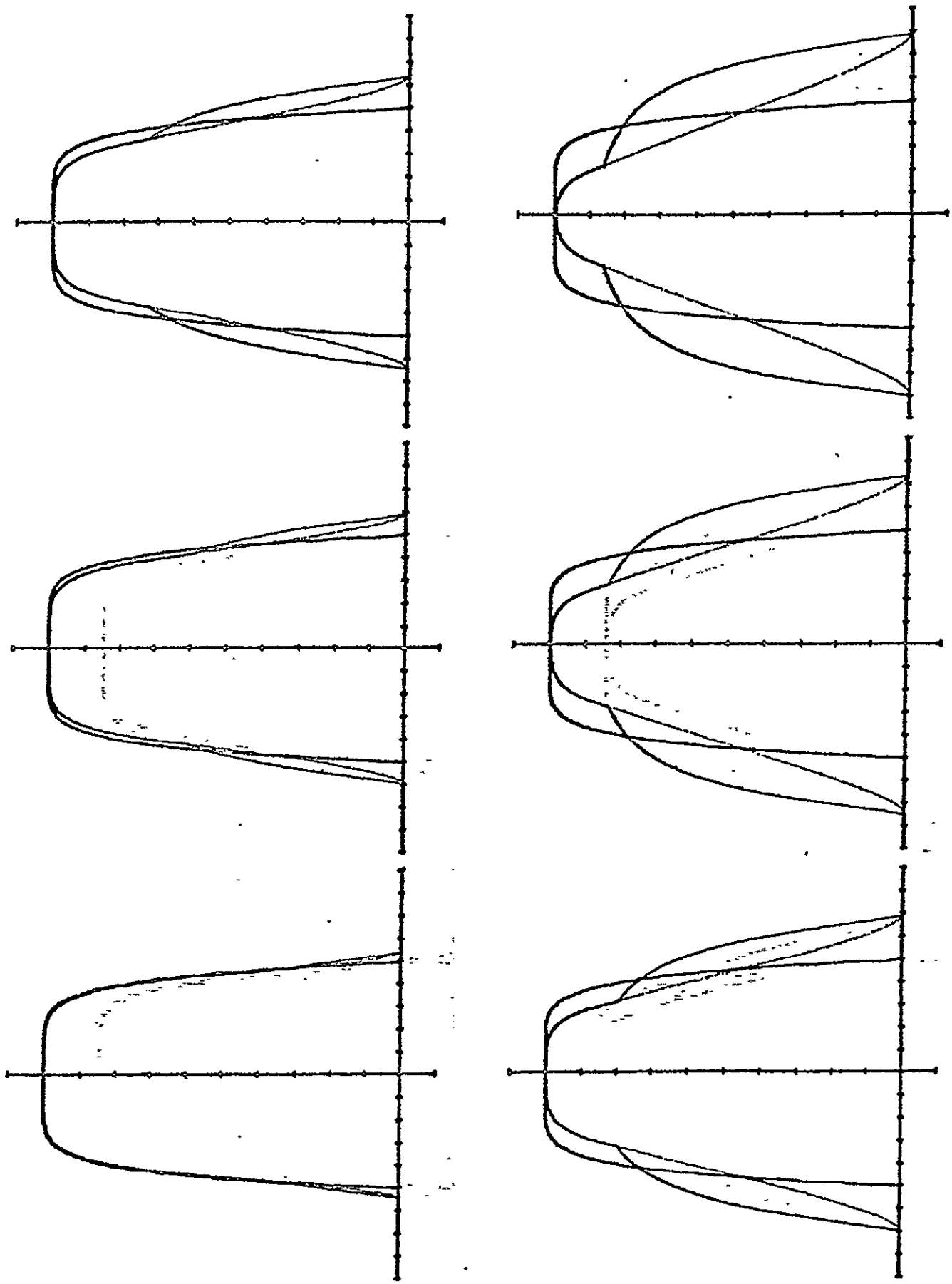

Fig. 2-11 Convolution and boundary error profiles for n=7.

to zero. This method is suitable for small sample function lengths, but obviously introduces rather large errors for lengths approaching the radius. An alternative method is to extrapolate the maximum and minimum profile slopes to zero velocity and take these points as the wall locations. This method reduces the error due to the convolution "tail" on the actual profile and allows wall determinations in noisy environments which disturb the baseline, but is also profile dependent and difficult to apply in irregular velocity fields. Occasionally, information on vessel diameter or wall locations is available from an independent source, such as radiographs or ultrasound power scans (to be described in later section). When such data is available, we can truncate our measured profiles to these new wall locations for purposes of calculating volume flow.

Taking into consideration the above methods for determining the vessel wall locations, volume flow was computed from the convoluted profiles and convoluted boundary error profiles six ways. For both profiles, flow was computed 1) over the entire width of the profile, 2) over the width of the in vessel profile, assuming an independent measure of the wall locations, and finally over a width determined by extrapolating the maximum and minimum profile slopes to the baseline The results are shown in Table 2-2 relative to the actual theoretical volume flow.

Since the convoluted velocity profile and the convoluted boundary error velocity profile represent bounds on the measured velocity profile, the volume flow calculated from these curves should also represent the range of computed volume flow. Figures 2-12 through 2-15 are graphs of the volume flow error range as a function of sample function length for various n values. Only two error ranges are graphed - that from computing the vessel wall locations from the maximum and minimum profile slope, and that from calculations using independent measurements of the wall locations which are assumed to be exact.

Volume Flow Comparisons

n	function length	volume flow	volume flow from convoluted profile		volume flow from conv. bound. error prof.		wall locations from profile slope	
			over actual diameter	complete	over actual diameter	complete	conv.	c.b.e.
2	.25	1.0	1.005	1.010	1.015	1.027	1.005	1.015
	.50	1.0	1.011	1.041	1.062	1.142	1.020	1.079
	.75	1.0	1.015	1.092	1.129	1.342	1.042	1.184
	1.0	1.0	1.018	1.162	1.207	1.621	1.110	1.415
	1.25	1.0	1.020	1.250	1.288	1.968	1.204	1.968
3	.25	1.0	1.003	1.008	1.014	1.029	1.003	1.014
	.50	1.0	.998	1.034	1.056	1.151	1.017	1.094
	.75	1.0	.989	1.078	1.111	1.358	1.051	1.252
	1.0	1.0	.977	1.138	1.170	1.637	1.108	1.637
	1.25	1.0	.963	1.214	1.227	1.978	1.188	1.978
5	.25	1.0	.999	1.007	1.014	1.033	.999	1.014
	.50	1.0	.983	1.029	1.050	1.171	1.014	1.118
	.75	1.0	.959	1.066	1.091	1.390	1.055	1.391
	1.0	1.0	.932	1.117	1.129	1.674	1.107	1.674
	1.25	1.0	.905	1.182	1.162	2.011	1.174	2.011
7	.25	1.0	.997	1.007	1.015	1.038	1.002	1.027
	.50	1.0	.973	1.027	1.047	1.188	1.021	1.188
	.75	1.0	.941	1.060	1.078	1.418	1.052	1.418
	1.0	1.0	.907	1.107	1.104	1.705	1.101	1.705
	1.25	1.0	.875	1.167	1.127	2.042	1.162	2.042

Table 2-2. Volume flow computations from theoretical velocity profiles. Values are normalized by volume flow from undistorted profile.

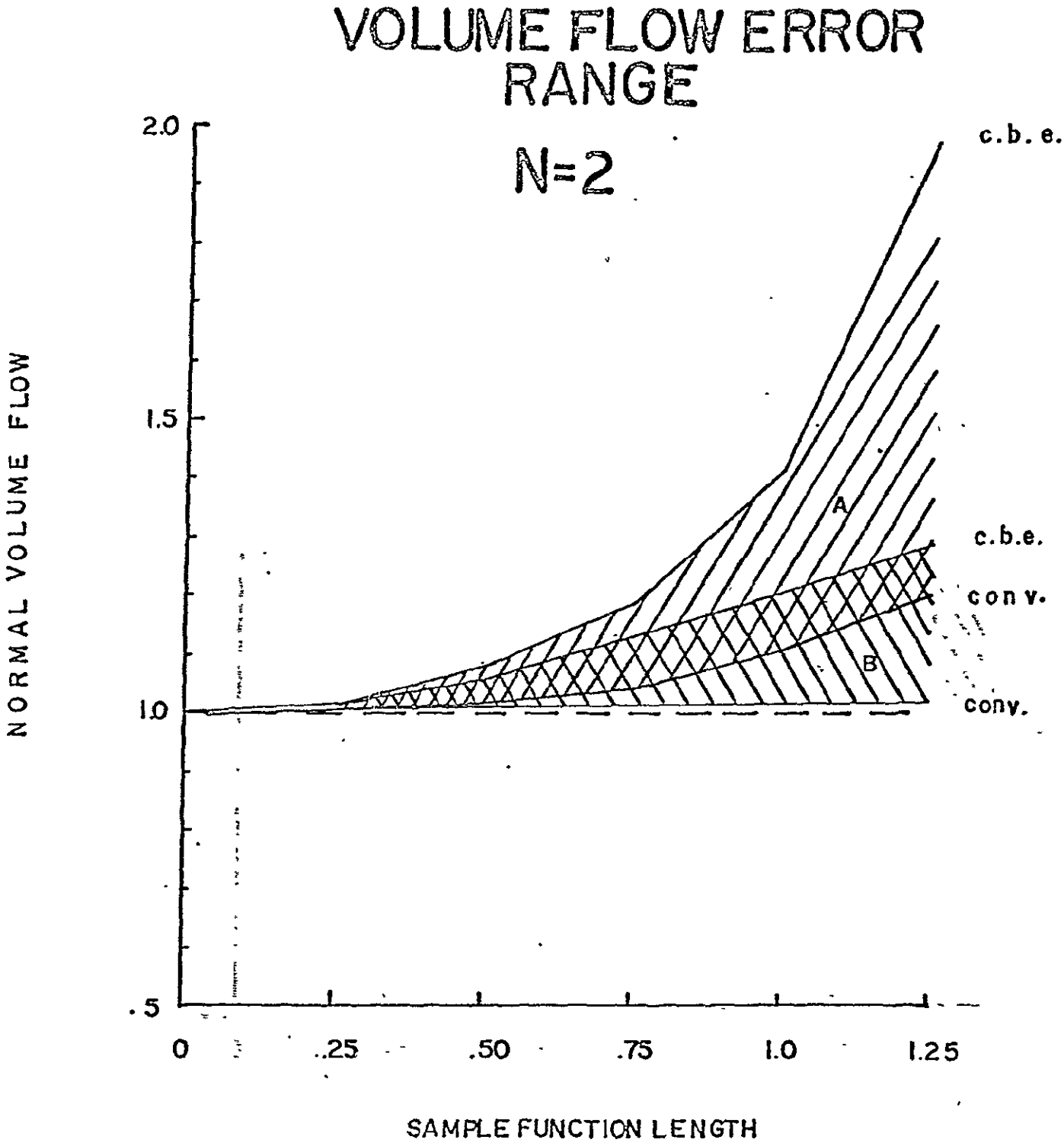

Fig. 2-12 Error range for computed volume flow for a parabolic velocity profile (n=2). Error range B applies when the wall locations are known exactly, and error range A applies if the wall locations are computed from the maximum and minimum profile slopes.

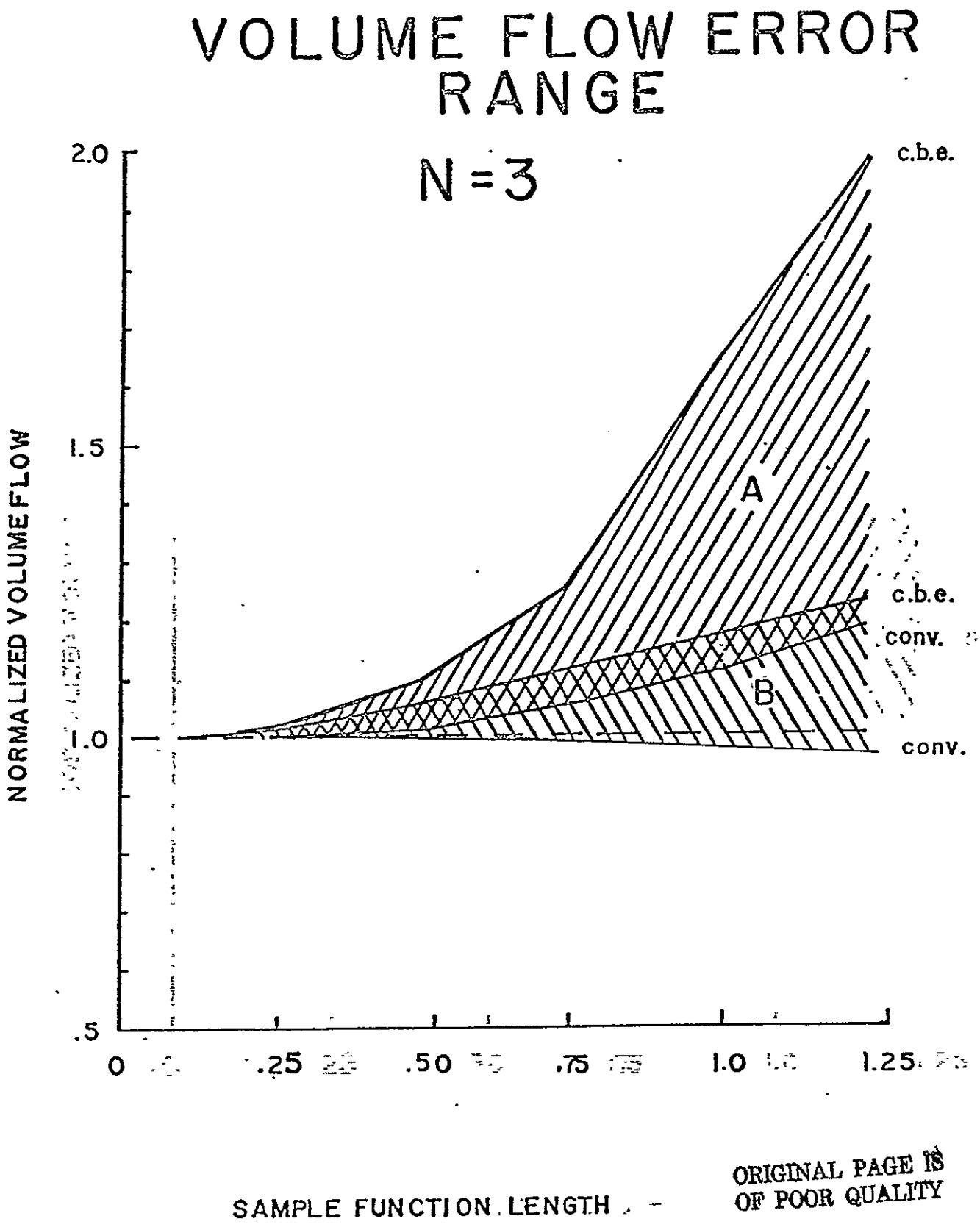

Fig. 2-13 Error range for computed volume flow from velocity profile of order n=3. Error ranges are as defined in Fig. 2-12.

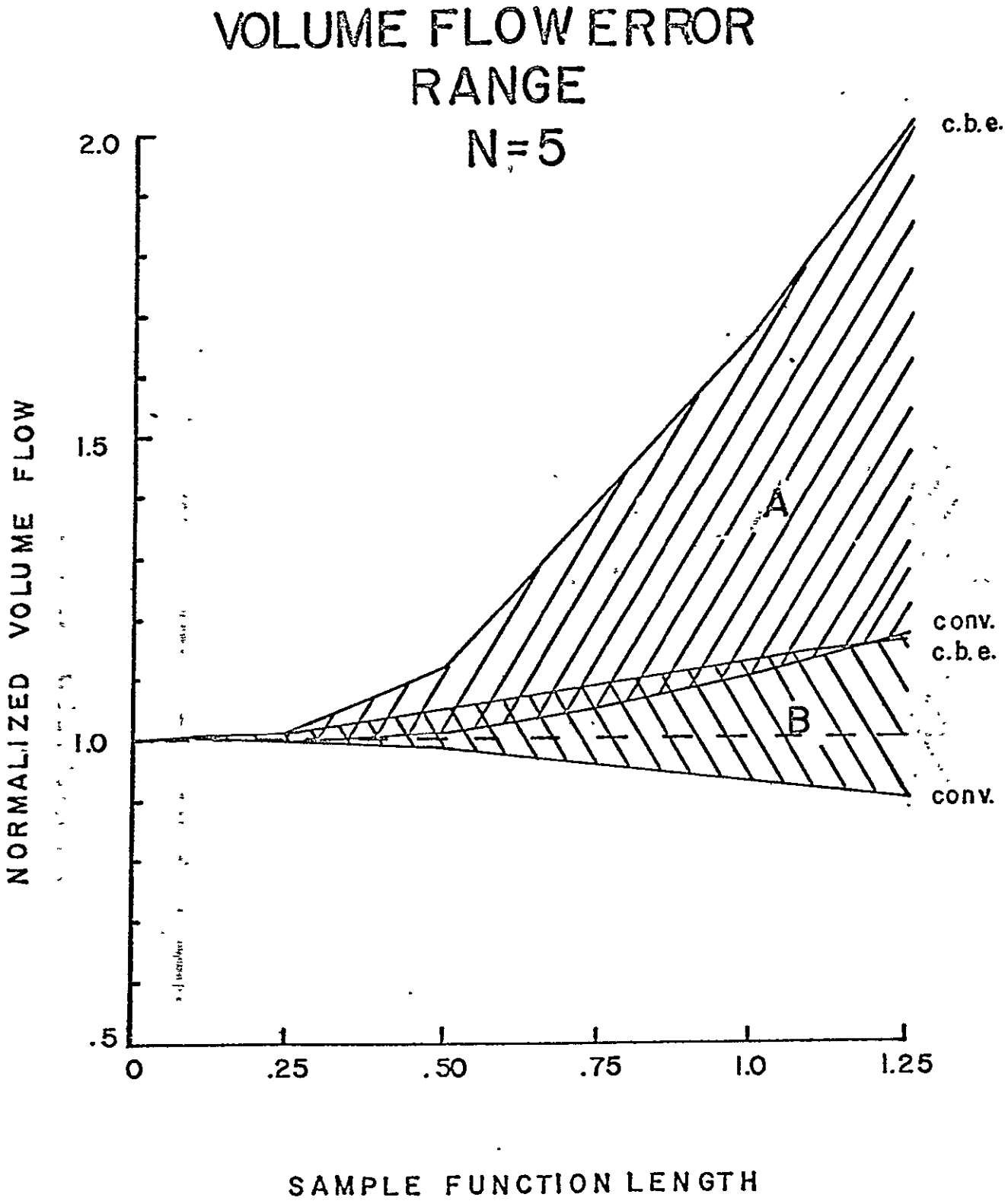

Fig. 2-14 Error range for computed volume flow from velocity profile of order n=5.

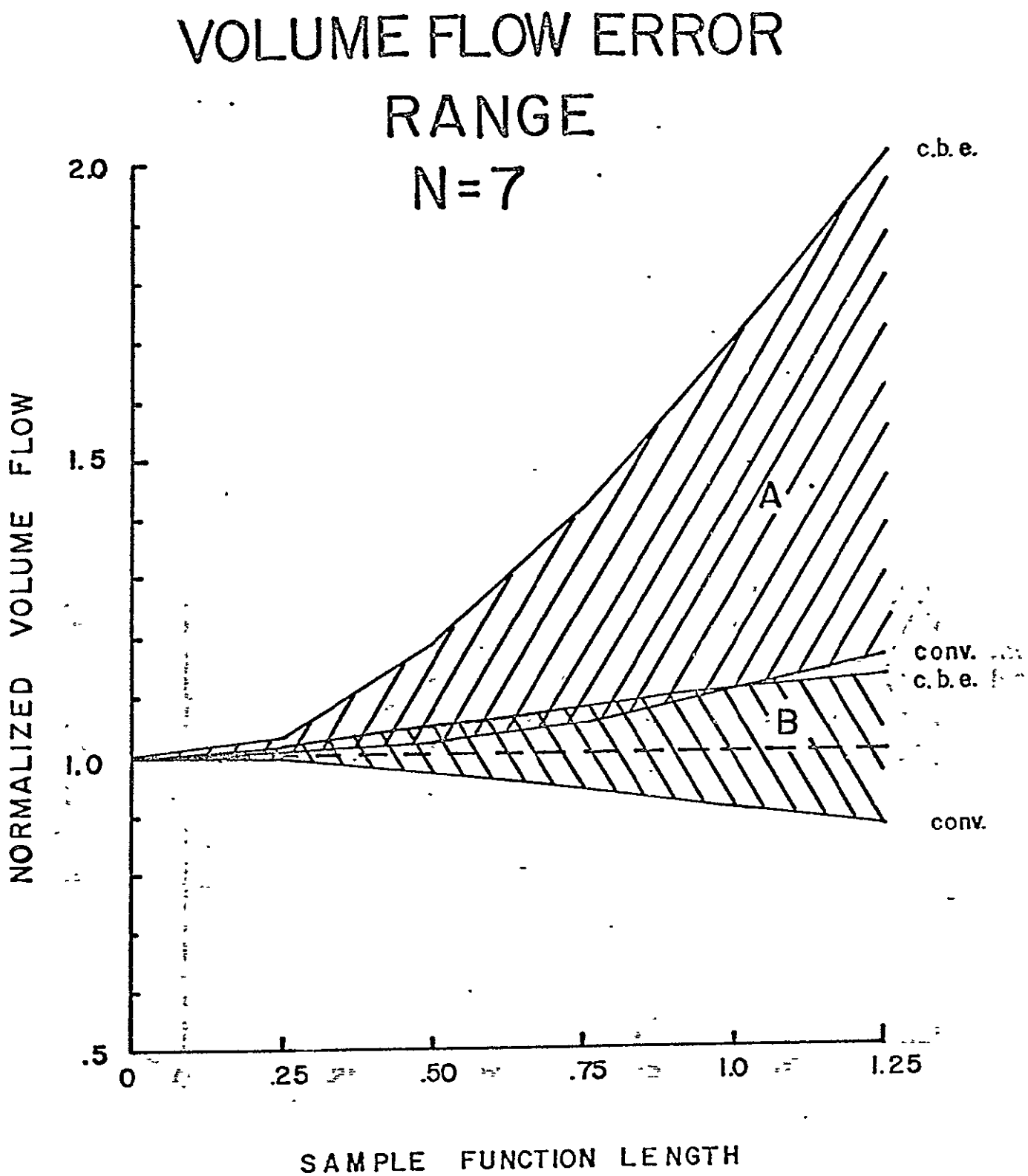

Fig. 2-15 . Error range for computed volume flow from velocity profile of order n=7.

As shown in Fig. 2-12 for the parabolic profile case, the error ranges are both above the normalized actual volume flow line of 1.0. As the sample function length is increased, the error ranges increase dramatically. Figures 2-13 through 2-15 show the same error ranges for higher values of n. Note that as n increases, the error range for the computer wall location volume flow increases more rapidly with increasing sample function length. Somewhat unexpectedly, however, the error range for volume flow, as calculated from the profiles with an independent measurement of the wall location, tends to remain constant with increasing n, and even moves down to symmetrically enclose the actual volume flow line.

Several conclusions can be made from the data in Figures 2-12 through 2-15. First of all, it is apparent that for sample function lengths less than .25r, the volume flow calculation from profile integration is quite accurate, regardless of the method of locating the vessel walls. Assuming a minimum practical sample function length of 1½ mm, the technique should be valid, from the standpoint of resolution, in vessels 12 mm in diameter and larger. Since most vessels that are accessible transcutaneously are considerably smaller than this, we must consider the situation of larger relative sample function lengths. For these situations, it is apparent that the method of determining the vessel wall locations from the profile slope can lead to rather large errors in volume flow, even with ideal profiles. It appears highly desirable to obtain an independent measurement of the vessel wall locations by some other more accurate technique. Finally, we see that accuracy depends, to some extent, on profile shape. For volume flow calculations based on profile slope measurements of wall locations, the error is likely to increase with increasingly blunt profile shapes. For the independent wall location technique, however, the error in computed volume flow is likely to decrease with blunt profile shapes.

Volume Flow Errors

Error Source	Magnitude
Velocity profile not across true diameter	~ cos (Doppler angle, σ)
Physiological variation during scan*	~ time required for scan
Non-cylindrical vessel	~ distortion in diameter
Non-symmetrical velocity profile	~ degree of skewing
Blood velocity vector not parallel to vessel axis	~ function of off axis angle, radius of vector and duration of error during cardiac cycle
Beam diameter, d too large for vessel radius, r	function of $\frac{d}{r}$, small for $\frac{d}{r} < .25$
Sound beam not aligned with vessel axis	~ $(\frac{\Delta r}{r})^2$ for uniform velocity field
Doppler angle error	~ $\frac{\cos\sigma}{\cos(\sigma+\Delta\sigma)} - 1$
Resolution errors	function of $\frac{\text{sample function length}}{\text{radius}}$ and of wall location method

*single gate PUDVM

Table 2-3. Errors in volume flow computed by diameter profile integration method.

Table 2-3 summarizes the error sources inherent in volume flow measurement by the diameter profile integration method. As shown in the table, this method is subject to probe alignment and geometry errors, asymmetrical velocity field errors and resolution errors. The magnitude of the geometry and resolution errors indicate that this technique is best suited for large blood vessels on the order of 10 mm diameter and above. The small size of subcutaneous vessels accessible to the PUDVM suggests that the profile integration technique is not suitable for accurate transcutaneous volume flow measurements.

3. Diameter gate average velocity method

This technique for obtaining volume flow is in effect a hybrid of the uniform illumination method and the diameter profile integration method. It has the advantages of the uniform illumination method in that it is simple and requires no computer processing. It shares with the diameter profile integration method the ability to measure vessel diameter with the same transducer used for velocity measurements. Unfortunately, the method also shares many of the error sources of both the other techniques.

The diameter gate average velocity technique utilizes a small transducer compared with the size of the vessel (again accuracy demands a transducer beam width $< .25r$). The transducer is oriented with respect to the vessel at a known Doppler angle so that the sound beam intersects the vessel axis. The gate of the PUDVM is then set to encompass the vessel lumen. If the flow characteristics are constant over the axial length of the vessel region under illumination, the average velocity along this thin sound beam represents the average velocity across the diameter of the vessel. If the gate is then narrowed and set to measure the peak velocity at the vessel centerline, the mean velocity for the whole vessel can be computed. A measurement of the diameter then allows calculation of total volume flow.

Equation 2.3 gives the mean velocity for the entire vessel cross-section for profiles of the form

$$v(r) = v_p\,(1-r^n) \qquad 0 \le r \le 1 \qquad 2.14$$

where $v_p = 1$. For v_p variable equation 2.3 becomes

$$\bar{v} = v_p\,\left(\frac{n}{n+2}\right) \qquad 2.15$$

The average velocity along a thin sample beam across a diameter is given by the integral

$$\bar{v}_c = v_p \int_0^1 (1-r^n)\,dr$$

$$\bar{v}_c = \bar{v}_p\left(\frac{n}{n+1}\right) \qquad 2.16$$

Solving for n in terms of $\bar{v}_c$ and v_p

$$n = \frac{\bar{v}_c}{v_p - \bar{v}_c}$$

Substituting the above equation for n in equation 2.15, we obtain the mean velocity in terms of $\bar{v}_c$ and v_p.

$$v = v_p\left(\frac{\bar{v}_c}{\bar{v}_c + 2v_p - 2\bar{v}_c}\right)$$

$$v = \frac{v_p \bar{v}_c}{2v_p - \bar{v}_c} \qquad 2.17$$

The above derivation is based on several assumptions. First of all, the velocity field is assumed to be axial symmetric, that is, the velocity profile

is constant with respect to rotation about the vessel axis. Secondly, the profile shape must be describable by the mathematical form given in equation 2-14. As for the diameter profile integration method, these assumptions preclude the applicatio of the method to skewed velocity fields.

Experimental errors inherent in the diameter gate average velocity technique are much the same as those for the diameter profile integration method. The transducer must be oriented at a known Doppler angle, minimizing the offset of the sound beam from the vessel axis. The beam diameter must be equal to or smaller than ¼ the radius. Care must be taken not to distort the vessel shape by excessive pressure on the probe.

Systematic errors are also involved, as with the other techniques. Since the Doppler shift spectrum is broad, due to the range of velocities present, errors in converting frequency to voltage using zero-crossing detection result. Using the same mathematical techniques employed for the uniform illumination method, we can obtain an estimate of the zero-crossing detection error. Applying equation 2.4 and integrating across a diameter we obtain

$$\bar{v}_m^2 = v_p^2 \int_0^1 (1-x^n)^2 \, dx$$

$$= v_p^2 \left[\frac{x^{2n+1}}{2n+1} - \frac{2x^{n+1}}{n+1} + x \right]_0^1$$

$$\bar{v}_m = v_p \left[\frac{1}{2n+1} - \frac{2}{n+1} + 1 \right]^{\frac{1}{2}} \qquad 2.18$$

Substituting $\bar{v}_m$ for $\bar{v}_c$ in equation 2.17, we obtain

$$\bar{v}_e = \frac{v_p \left[\frac{1}{2n+1} - \frac{2}{n+1} + 1 \right]^{\frac{1}{2}}}{2 - \left[\frac{1}{2n+1} - \frac{2}{n+1} + 1 \right]^{\frac{1}{2}}} \qquad 2.19$$

The actual $\bar{v}$ is given by equation 2.15. Dividing $\bar{v}_e$ by $\bar{v}$ gives the normalized error.

$$\frac{\bar{v}_e}{\bar{v}} = \frac{n+2}{n} \cdot \frac{\left(\frac{1}{2n+1} - \frac{2}{n+1} + 1\right)^{\frac{1}{2}}}{2 - \left(\frac{1}{2n+1} - \frac{2}{n+1} + 1\right)^{\frac{1}{2}}} \qquad 2.20$$

The error in computed volume flow is similar to the normalized mean velocity error and is plotted as a function of n in Fig. 2-16. Note the similarity between Fig. 2-16 and Fig. 2-1 which gives the normalized volume flow error introduced by the zero-crosser for the uniform illumination method. The two curves are nearly identical, even though the equations from which they are derived are quite different in form.

This similarity in the volume flow error introduced by zero-crossing detection for the diameter gate average velocity and uniform illumination methods suggests an interesting possibility. If the peak velocity and mean velocity are known, it is possible to compute n from equation 2.15 or equation 2.18, depending on the method in use. Knowing n, it is then possible to correct the zero-crossing error using the curve in Fig. 2-1 or Fig. 2-16. While this involves some rather complex processing, the error in volume flow can potentially be eliminated.

Other systematic errors involved in the diameter gate average velocity method are due to resolution errors. The error in diameter measurement has a considerable effect on calculated volume flow and the remarks in section 2.1 apply. Fig. 2-3 shows the percent error in volume flow introduced by diameter measurement errors.

Table 2-4 lists the error sources associated with the diameter gate average velocity method. The large number of experimental and systematic error sources raise doubt as to the accuracy of this technique, especially in small vessels

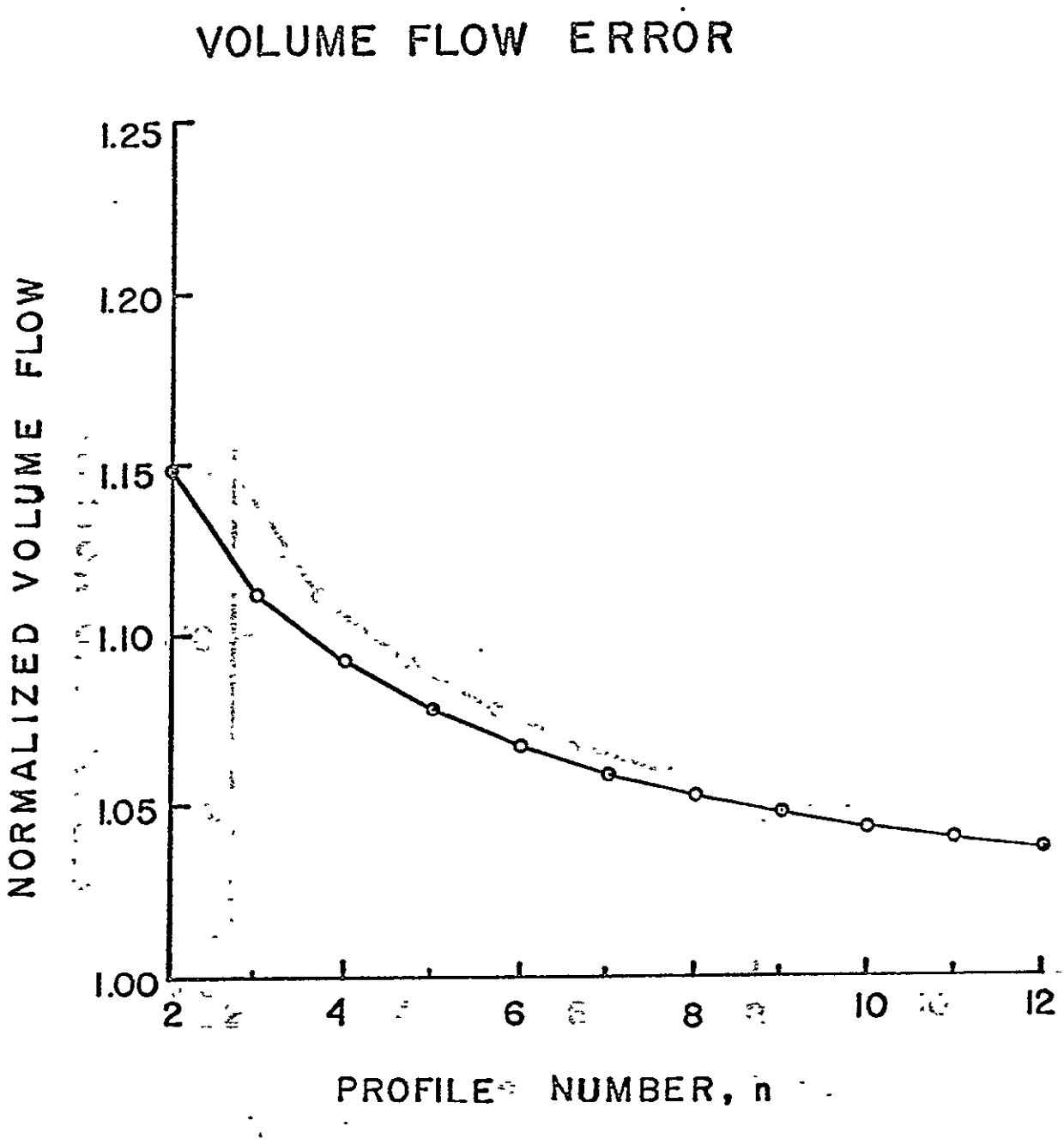

Fig. 2-16 Volume flow error introduced by zero-crossing detection for core sample average velocity method.

Error Source	Magnitude
Measured velocity not across true diameter	~ velocity variation along vessel
Non-cylindrical vessel	~ distortion in diameter
Non-symmetrical velocity profile	~ degree of skewing
Blood velocity vector not parallel to vessel axis	~ function of off axis angle, radius of vector and duration of error
Beam diameter, d, too large for vessel radius, r	function of $\frac{d}{r}$; small for $\frac{d}{r} < .25$
Sound beam off vessel axis by Δr	~ $(\frac{\Delta r}{r})^2$ for uniform velocity field
Doppler angle error	~ $\frac{\cos\sigma}{\cos(\sigma+\Delta\sigma)} \simeq 1$
Zero-crossing detection error	see Figure 2-16
Resolution error in diameter measurement	~ $\frac{2\Delta d}{d} + (\frac{\Delta d}{d})^2$

Table 2-4. Error source in volume flow determination by diameter-gate average velocity method.

with skewed velocity fields. The method's greatest advantage lies with the ability to obtain volume flow estimates with a narrow beam width transducer without computer processing of profile data. Since the same small transducer may be used to obtain a vessel diameter estimate, all essential data for computing volume flow can be acquired from a single transducer element, suggesting the possibility of multiplexing schemes. Such complex types of data acquisition and processing are still in the future.

III. Resolution Studies

The resolution of the PUDVM in making blood velocity measurements is an important factor in velocity profile studies. In section 2.2 the effect of limited axial resolution along the sound beam on velocity profile measurements and derived volume flow calculations was demonstrated. The other methods of volume flow determination involve vessel diameter measurements, which when made with the PUDVM, are also subject to resolution errors. Resolution, therefore is an important consideration in pulsed ultrasonic blood flow measurements.

1. Theoretical aspects

The ability of the PUDVM to resolve spatial velocity distributions is defined by a measurement function which describes the geometric region over which the distribution is sampled and averaged by the measurement process. The dimensions of the sample region vary with experimental conditions and are characterized by the transducer radiation pattern, length of emission pulse, transducer and receiver bandwidths and sample gate time. The transducer radiation pattern generally defines the width of the sample region, while the other parameters influence the axial length. For velocity profile measurements the critical dimension is the projection of the sample region length on the diameter of the vessel under study, which introduces an additional factor - the Doppler angle. Fig. 3-1 illustrates how these individual elements of resolution combine to generate the measurement function, referred to as the sample function.

Analytically, the sample function can be derived by considering reflections from a line source of scatterers transversing the transducer field. Experimentally, the function can be observed as the power returned from a moving line or sheet of flow. For purposes of illustration and in an attempt to make some general

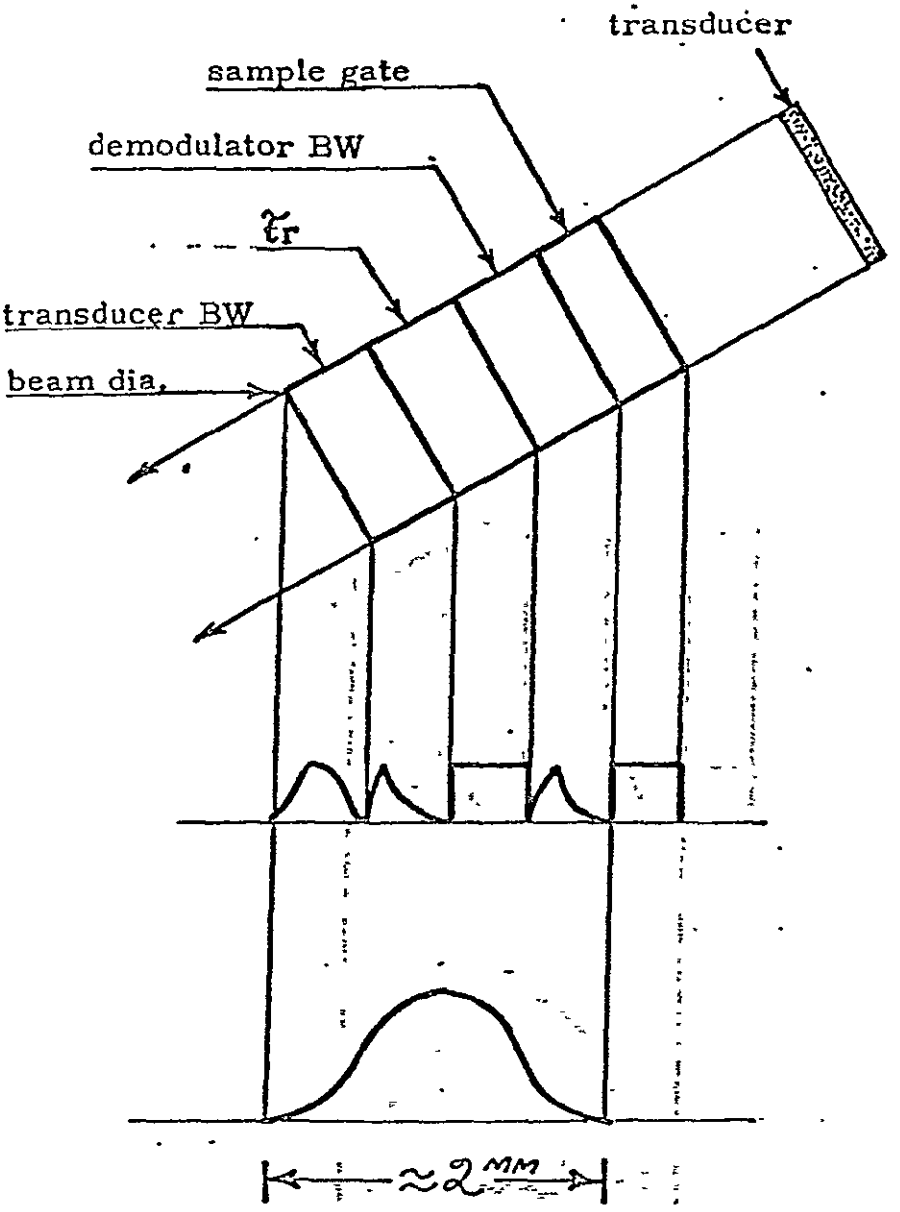

Fig. 3-1 Elements contributing to sample function of the PUDVM.

statements regarding the sample function, the transducer beam is assumed to be of constant cross-section in the region of the sample function. This approximation requires a slowly diverging beam, as in the case of a transducer several wavelengths in diameter.

The power scattered and returned to the transducer by a reflector is proportional to the illuminating power, the scattering cross-section, and the transducer gain in the direction of the reflector. Thus, for a common emission and reception transducer the return power can be expressed as:

$$P(R,r,t) = \sigma G^2(R,r)Pe(t - \tau)$$

where σ = scattering cross-section

G = transducer power gain

Pe = emission power

R = range

c = velocity of sound

τ = range delay

Referring to Fig. 3-2, the transducer gain can be written in the form

$$G(R,r) = G\left(\frac{\gamma_o}{\sin\alpha}, x \sin\alpha\right)$$

In terms of range delay τ_r this becomes

$$G = G\left(R_o, \frac{c\tau_r}{2} \frac{\sin\alpha}{\cos\alpha}\right)$$

Similarly the emission power Pe becomes

$$Pe\left(t - \frac{2}{c}\frac{\gamma_o}{\sin\alpha} - \frac{2}{c} x \cos\alpha\right) = Pe\left(\tau' - \frac{2}{c} x \cos\alpha\right)$$

The term $\frac{2}{c} x \cos\alpha$ is simply the range delay τ_r in the x direction, thus

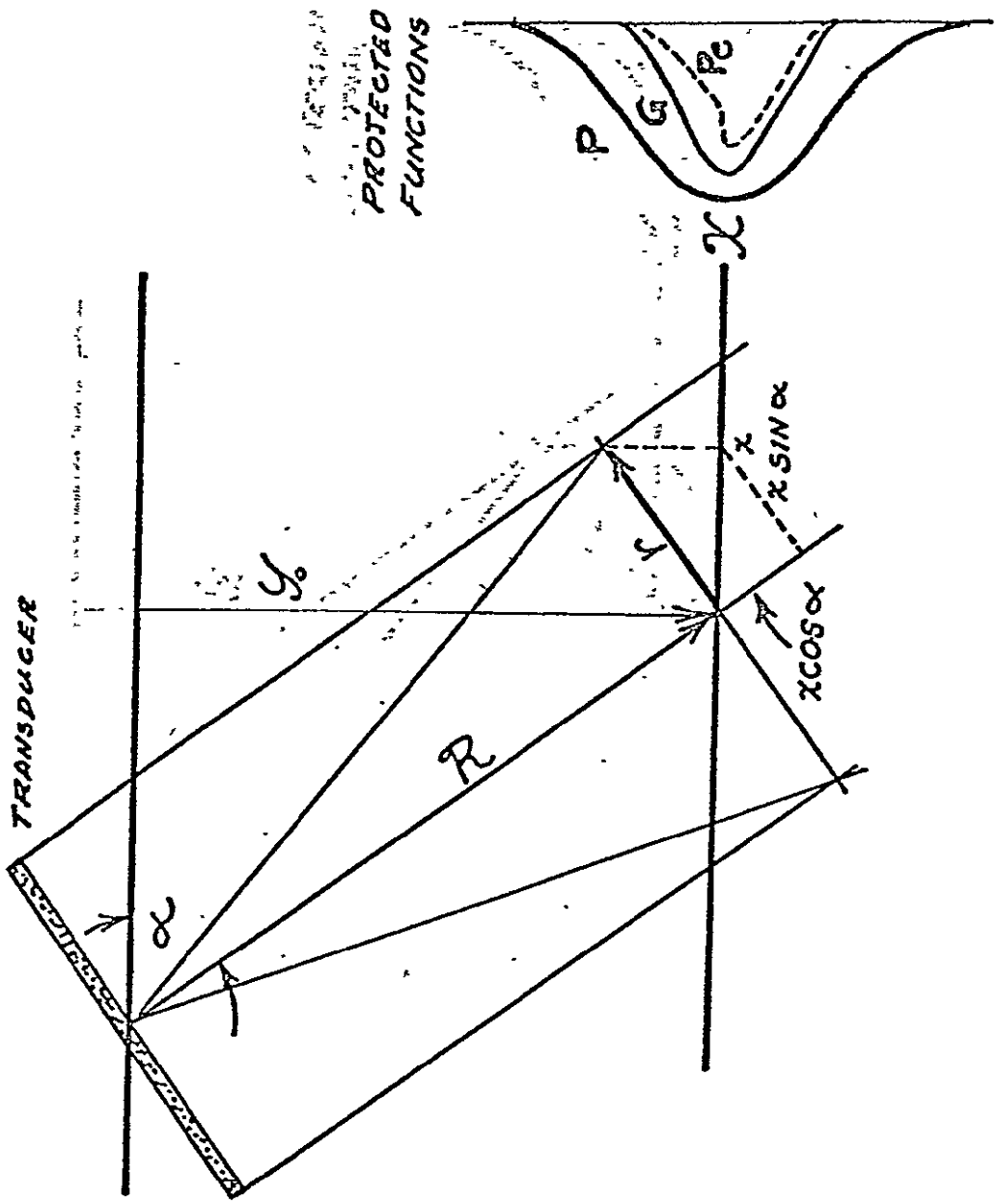

Fig. 3-2 Geometry of sample region.

$$Pe(\tau' - \frac{2}{c} x \cos\alpha) = Pe(\tau' - \tau_r)$$

The total returned from the plane of scatters at $\tau_o = \frac{2R}{c}$ is simply the integral of the scattered power over the entire plane

$$Px = \int G(R_o, \frac{c}{2}\frac{\sin\alpha}{\cos\alpha}\tau_r)\ Pe(\tau_o - \tau_r)dx$$

$$= \frac{c}{2\cos\alpha} \int G(R_o, \frac{c}{2}\frac{\sin\alpha}{\cos\alpha}\tau_r)P(\tau_o - \tau_r)d\tau_r$$

which is recognized as the convolution of the emission power pulse with the projected transducer gain pattern. The effect of limited transducer and or system bandwidth is readily incorporated in this expression by defining Pe as the signal one would record from an ideal point reflector rather than on the rectangular excitor burst. Typically, limited transducer bandwidth adds about ½μ sec to the emission burst. Limited demodulator bandwidth also tends to stretch the pulse making a broadband (5 MHz) demodulator imperative.

Signals reflected from a desired depth are selected by range gating the return signal P_x. The range or sample gate, described by the function a(t), has unity transmission during the selected sample interval, τ_g, and zero transmission at all other times. Low pass filtering of the gated signal retains only the zero order frequencies, thus the gate output P becomes

$$Po(\tau - \tau_o) = \int P(\tau - \tau_o)a(\tau)d\tau = \int_{\tau_o - \frac{\tau_g}{2}}^{\tau_o + \frac{\tau_g}{2}} P(\tau - \tau_o)d\tau$$

The form of this expression is also recognized as a convolution integral. Substituting and combining terms the range resolution or sampled function becomes

$$h(x) = g*Pe*a$$

Expanding the emission power Pe in terms of the excitor pulse P, the transducer bandwidth b and demodulator bandwidth d

$$Pe = p*b*d$$

Thus h(x) becomes

$$h(x) = g*p*b*d*a$$

Or in terms of spatial frequency, s

$$H(s) = GPDA$$

The expression of the sample function as the convolution of the component parts leads directly to the observation that the overall length of the sample function is given by the sum of the component widths and the realization that each component tends to low-pass filter the spatial velocity distribution.

The sample function can be measured experimentally as an impulse or step response. The impulse response is the signal level recorded from a thin flow sheet as a function of range. The step response is equal to the integrated impulse response and is the signal level recorded as the sample region is slowly moved from a region of zero flow into the velocity field (see Fig. 3-3).

Experimentally the step response is much more easily obtained than the impulse response and can be directly evaluated at the time of experiment. The difficulties and uncertainties associated with maintaining a thin (= .1 mm) flow test section are eliminated. The only experimental constraint is that the step be abrupt compared to the resolution of the system being tested. Worst case abruptness of the experimental test function can be estimated from the minimal velocity to which the instrument will respond and the velocity gradient dv/dr at the wall

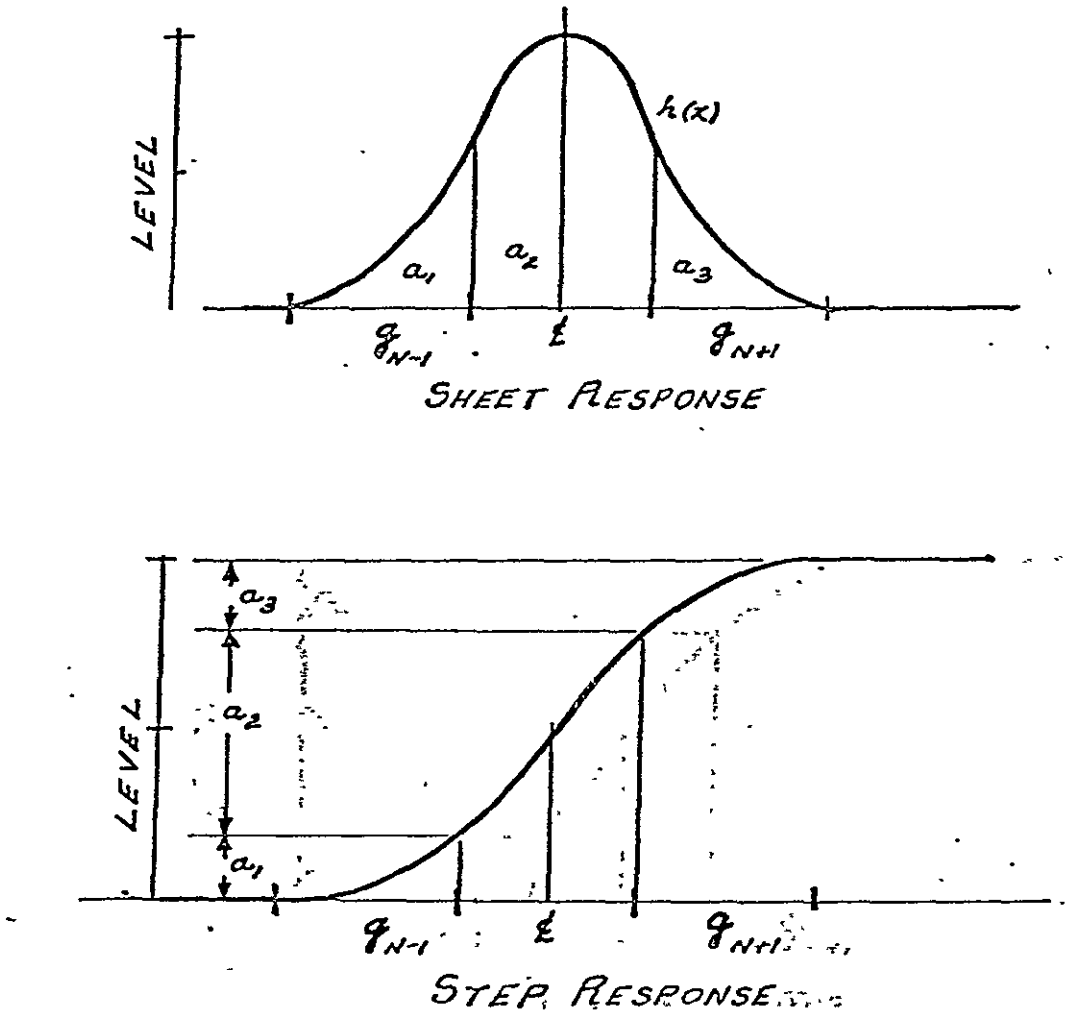

Fig. 3-3 Sheet and step response of the PUDVM. The 3dB level points for each curve are indicated.

$$\Delta = \frac{Vmin}{\frac{dv}{dr}\Big|_{r=R}}$$

For the present discussion a parabolic velocity profile is taken as the worst case. Turbulent and oscillatory profiles tend to be blunter and therefore have a steeper velocity gradient and can thus be regarded as providing a steeper step. The velocity distribution for parabolic flow is

$$V = V_0(1 - (\frac{r}{R})^2)$$

where V_0 is the peak velocity and $\frac{r}{R}$ is the nondimensional radius. The velocity gradient at $\frac{r}{R}$ equal to one is

$$\frac{dV}{d(\frac{r}{R})}\Big|_{\frac{r}{R}=1} = -2V_0$$

The minimal sensable velocity of the present instrument is on the order of 1 cm/sec. A typical V_0 is .5 m/sec. Substituting the abruptness of the step ΔR becomes

$$\Delta(\frac{r}{R}) = \frac{1}{100}$$

The 1/100 fractional radius step abruptness is for steeper than the instrument resolution and can therefore be considered ideal.

Next to resolution, the most serious limitation of the Doppler flowmeter is its inability to detect zero flow. As a consequence of this the sample function changes as it is scanned across the vessel wall into a region of zero flow. This boundary error produces profile broadening and distortions in excess of those produced by convolution alone. The effect is particularly troublesome in velocity gradient and shear stress studies.

A correction factor for this effect can be derived by applying appropriate limits to the convolution integral. The desired velocity V_d for a sample function located near the wall is given by

$$V_d = \frac{\int_{-\infty}^{\infty} P(x)V(x)dx}{\int_{-\infty}^{\infty} P(x)dx}$$

However outside the vessel wall, $x \geq \gamma$, the velocity is zero and the power contributed from this region is also zero. Therefore:

$$V_m = \frac{\int_{-\infty}^{\gamma} P(x)V(x)dx}{\int_{-\infty}^{\gamma} P(x)dx}$$

Since $V(x)$ is zero for $x \geq \gamma$ the numerator of V_d and V_m are equal to

$$\int_{-\infty}^{\gamma} P(x)V(x)dx = \int_{-\infty}^{\infty} P(x)V(x)dx$$

Subsequently the desired velocity V_d becomes

$$V_d = \frac{\int_{-\infty}^{\gamma} P(x)dx}{\int_{-\infty}^{\infty} P(x)dx} V_m$$

Thus the boundary error is readily related to the sample function. The appropriate correction factor is merely the fraction of the sample function remaining within the flow stream. For the case of a symmetrical sample function centered at the wall, the correction is 0.5 and independent of $P(x)$.

2. An apparatus for studying the sample region of the PUDVM

Due to the many factors influencing the extent of the sample region of the

PUDVM, experimental determination of the sample function is often necessary for obtaining an estimate of the measurement resolution. As mentioned in the previous section, the impulse response can be determined using a moving sheet of flow giving the sample function directly. Alternatively, the step response can be measured by moving the sample region into a uniform field of flow. Both of these methods require rather careful experimental set ups and precise measurements.

Since the sample region is defined by a spatial distribution of acoustical power, reflected energy from stationary targets can also be used in studying the extent of the region. If a small, dense spherical object, such as a steel ball bearing is placed in radiation field of an ultrasonic transducer, it approximates a point reflector of acoustical energy. For the PUDVM, this reflected energy can be received during the time between emission pulses and processed by a squaring circuit to obtain a measure of received power. Further processing by the sample gate of the PUDVM allows all elements influencing the extent of the sample region to exert their effects. By moving the reflector through the sample region, power maps can be made and the dimensions of the region can thus be defined.

A schematic diagram of a testing apparatus based on the above concepts is shown in Fig. 3-4. The transducer and ball bearing are located in a water bath with the ball bearing movable in three dimensions. Two of the dimensions, in the axial beam direction and across the beam path, can be measured using slide-wire potentiometers either of which can provide a voltage drive to an X-Y recorder. The basic circuitry of the PUDVM is employed, except the demodulator is connected as a squaring circuit with the receiver signal applied to both input ports. The output of the sample gate drives the other input of the X-Y recorder.

The testing apparatus can be used in a number of different studies of acoustical intensity distributions. Since the radial extent of the sample region

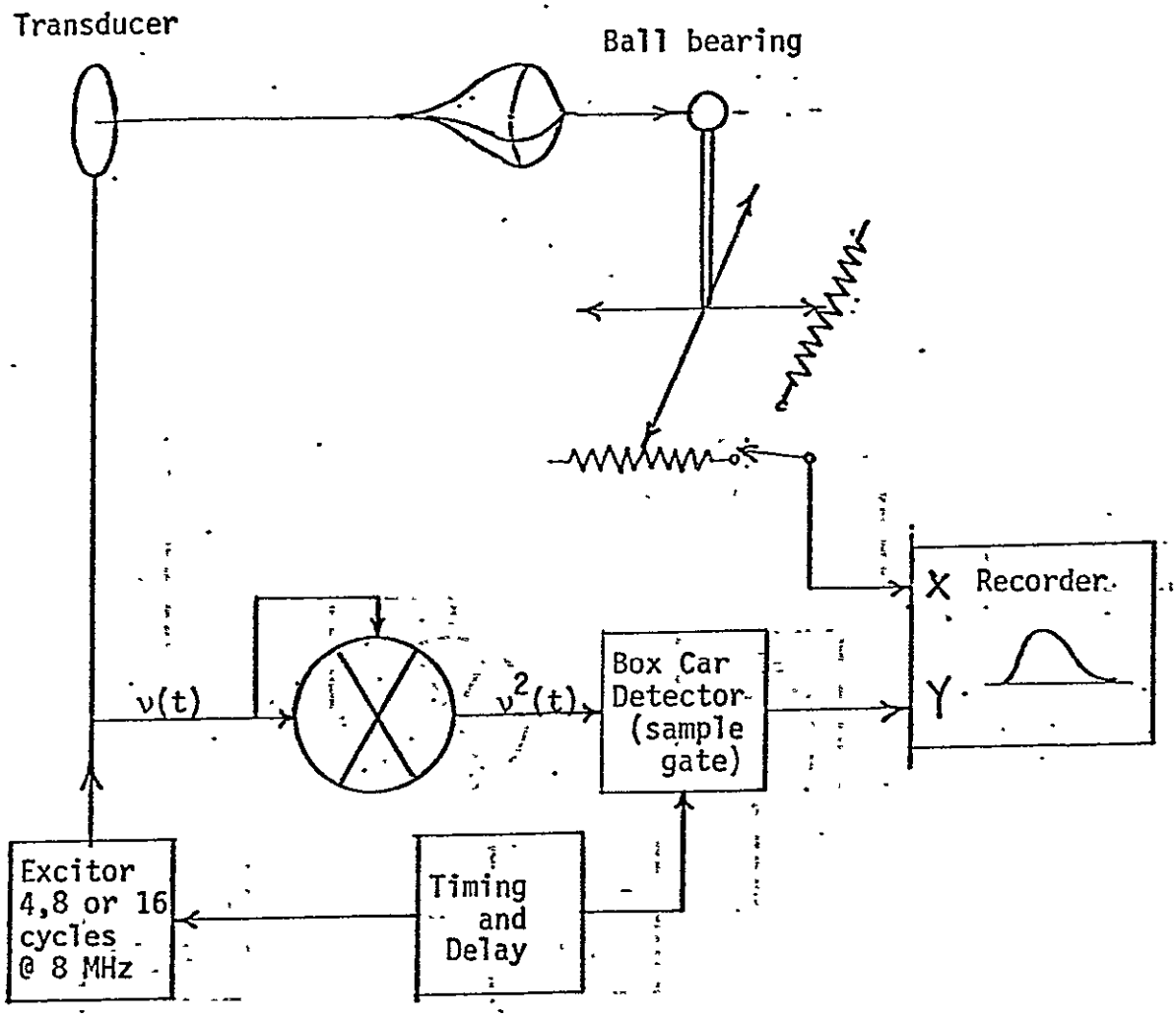

Fig. 3-4 Transducer beam and sample region mapping apparatus.

is determined by the radiation pattern of the ultrasound tranducer, this pattern can be mapped by positioning the sample region at various distances from the transducer face (by changing the delay time between emission and sample gate) and scanning the ball bearing through the center of the region in a cross-beam direction. Such a map is shown in Fig. 3-5 for a 1.5 mm circular transducer. Note the attentuation in received power as a function of range and the slight beam divergence. Such maps can be useful in assessing the quality and useful range of a given transducer.

A more significant use of the testing apparatus is in the mapping of the sample region of the PUDVM and studying the influence of various elements on the extent of this region. Fig. 3-6 shows the results of an axial scan of the ball bearing through the sample region for two emission pulse durations. The power curve thus obtained provides an accurate description of the sample function (the actual sample function is obtained by projection onto the vessel diameter and is dependent on the Doppler angle). Such axial power scans are useful in investigating the changes in the sample function with range. Primarily, however, they are used in determining the effects of parameters such as pulse lengths, transducer and receiver bandwidth, and gate time on the axial length of the sample function. Many of these effects are documented in the next section.

The testing apparatus described should prove useful to any investigator working with pulsed ultrasound devices. It can be used to investigate transducer characteristics alone, such as efficiency, Q and focusing properties. It can also be used to determine the sample region of a PUDVM, thereby giving the investigator accurate knowledge as to the resolution of his instrument.

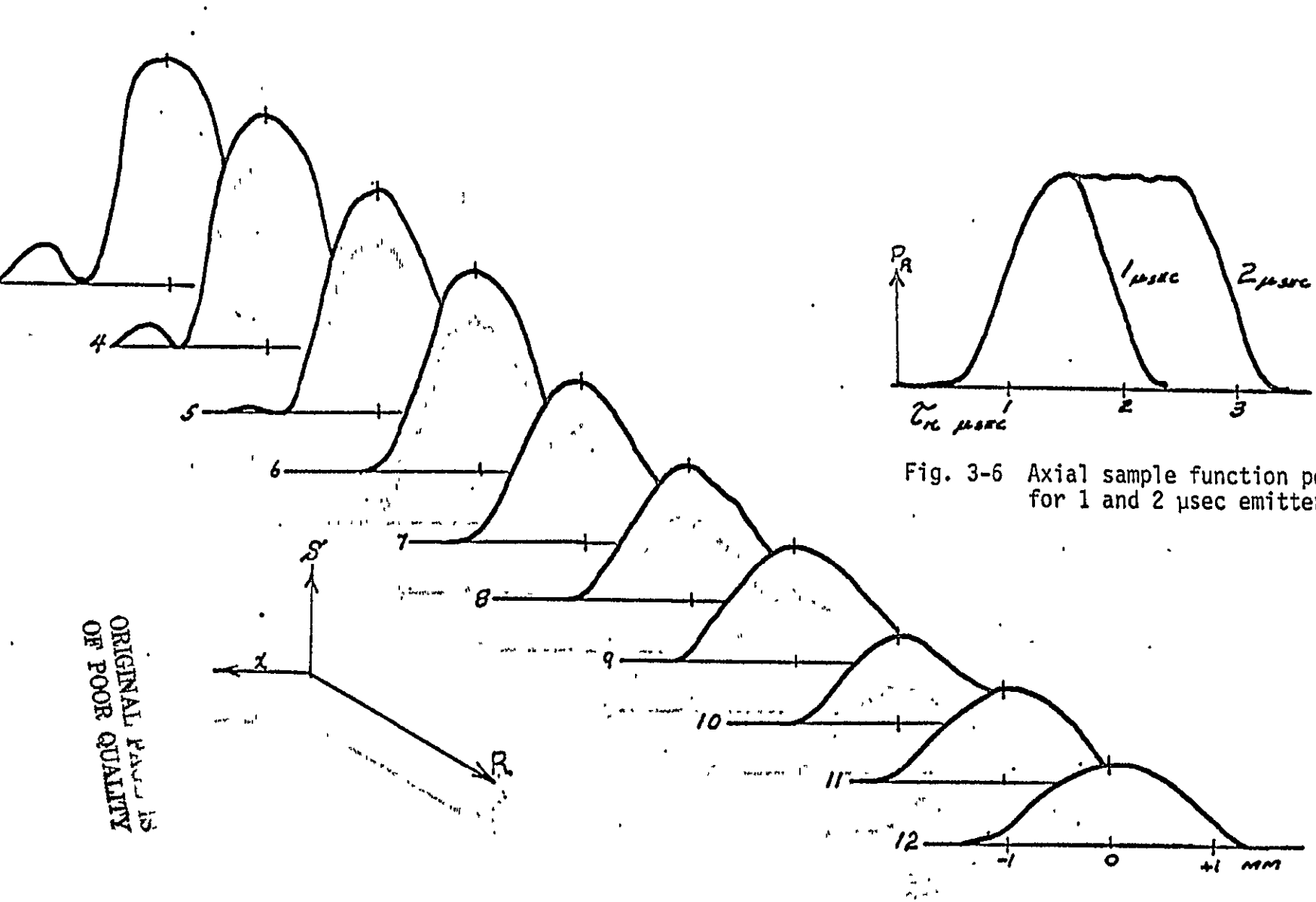

Fig. 3-5 Cross-sectional beam power as a function of range for a 1.5 mm transducer.

Fig. 3-6 Axial sample function power for 1 and 2 μsec emitter durations.

3. Experimental measurement of sample function effects

To obtain more specific information on the resolution of the PUDVM under various experimental and technical conditions, the testing apparatus described in the previous section was used to measure sample function power along the sound beam axis. These measurements can be made in either of two ways. One method is to set the sample region at a given distance from the transducer face by varying the range delay and then move the ball bearing axially through the region to map the sample function. Alternatively, if the PUDVM has a level output proportional to range delay, this output can be used to drive the X axis of the recorder and the ball bearing can remain fixed while the range delay is varied to move the sample region. This latter method was found to be more convenient and consequently, the X axis of most of the plots to be presented is calibrated in terms of range delay in microseconds, rather than distance. The delay times may be converted to distance in millimeters by multiplying times the conversion factor, .75 mm/μsec.

One of the most significant factors in specifying the radial extent of the sample region is the emission pulse length. The electrical pulse delivered to the transducer generally consists of several cycles at the frequency of the emission oscillator. The transducer response tends to round the leading and trailing edges of this pulse in the conversion to acoustical energy. Several factors are involved in the transducer response, including Q of the transducer material and the manner in which it is mounted. Figs. 3-7 through 3-9 illustrate typical sample functions obtained for various pulse lengths, τ_r, and transducer backing materials. Fig. 3-7, for example shows the sample function produced at various pulse lengths for a circular piezoelectric crystal (lead-titanate-zirconate) mounted by its outer perimeter only. Note the smoothness of the sample function shape. Only for τ_r = 2μsec does the transducer obtain its full output power. Figs. 3-8 and 3-9

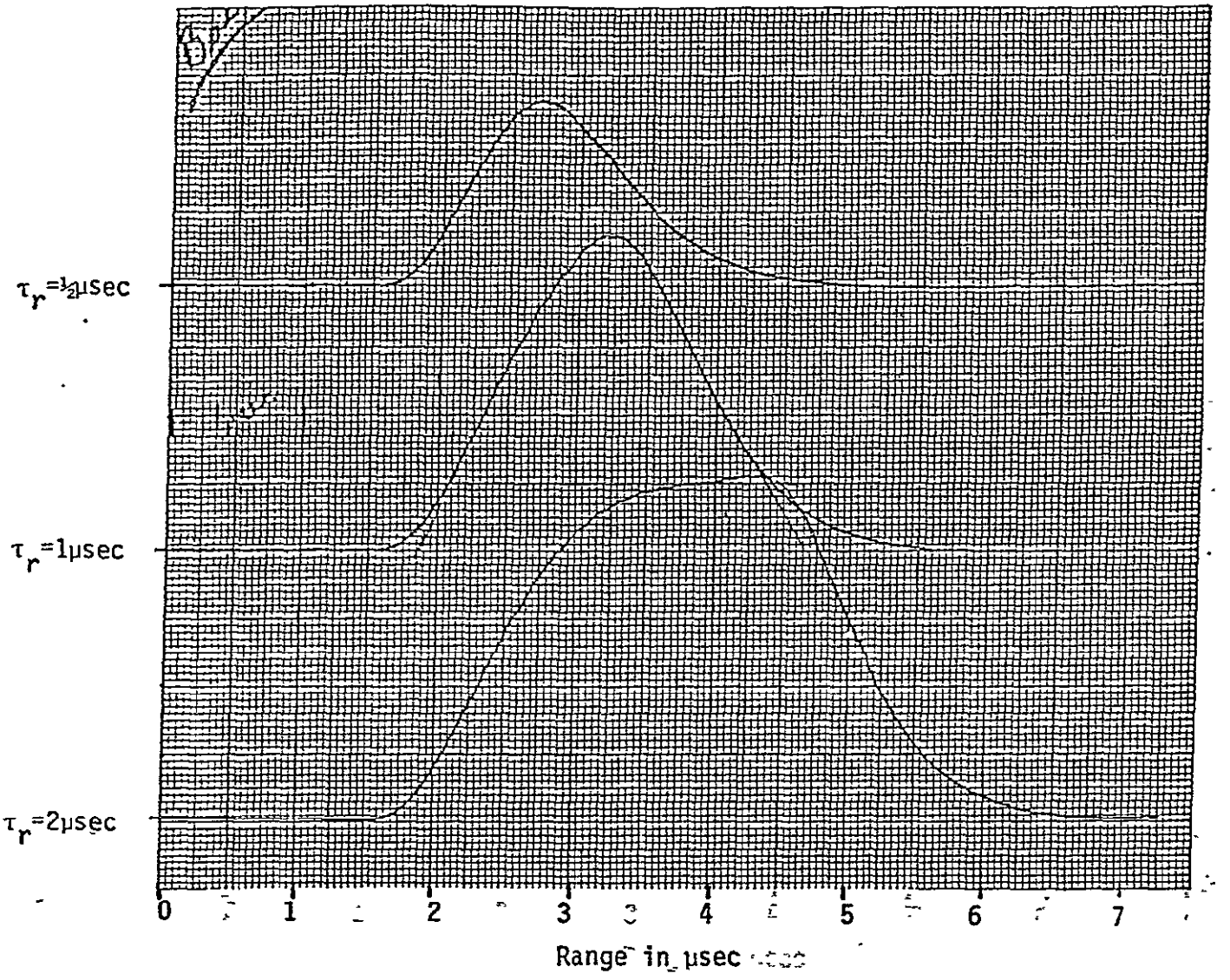

Fig. 3-7 Effect of transmitter duration time on sample function length for air-backed transducer.

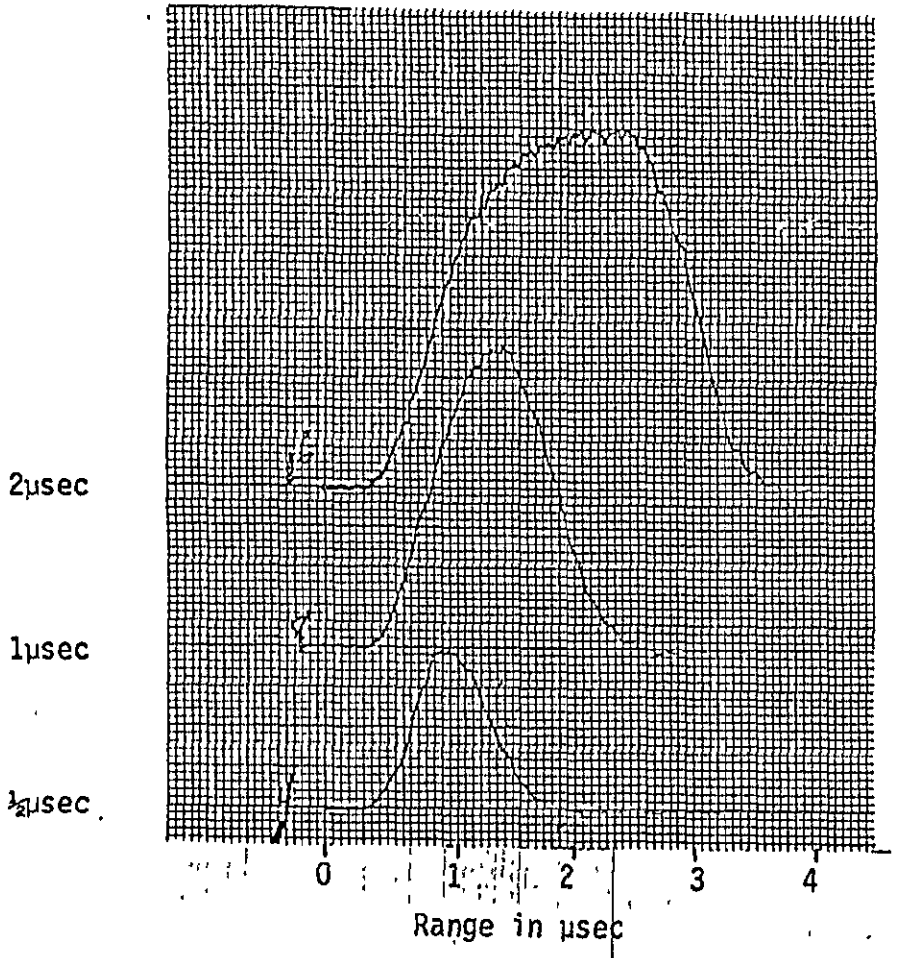

Fig. 3-8 Sample function length at different emitter durations for styrofoam backed transducer.

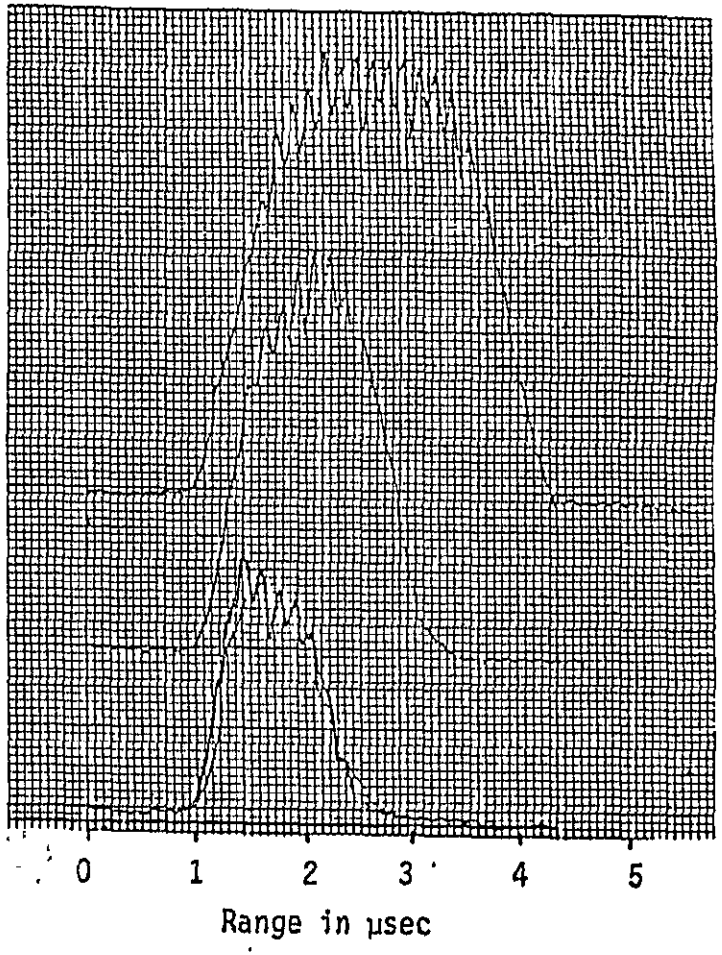

Fig. 3-9 Sample function lengths for "5-min." epoxy backed transducer.

show similar curves for other types of transducer backings. The curves in Fig. 3-9 for 5-minute epoxy backing show irregularities due to reverberations off of air bubbles in the epoxy medium and demonstrate the need for an acoustically quiet backing material.

Another factor which has a significant effect on sample function length and shape is the bandwidth of the ultrasound receiver section of the PUDVM. Early designers sought to reduce the effect of extraneous noise sources by limiting the pass band of the receiver to cover the Doppler sidebands only. This band-limiting is appropriate for continuous wave Doppler flowmeters, but has the undesirable effect of decreasing resolution for the PUDVM. This can be seen by considering the frequency domain transform of the emission pulse. For a continuous wave sound beam, the transform is an impulse at the emission frequency. For a burst of the emission frequency, however, the transform is a sin w/w type function centered at the emission frequency. The shorter the emission pulse, the broader the transform and for a pulse of 1μsec duration, the width of the main lobe of the sin w/w function is 2 MHz. The receiver bandwidth must be broad enough to cover at least this range of frequencies for high resolution measurements.

The effect of limited receiver bandwidth is to stretch out the sample function in the axial direction. This effect is demonstrated in Fig. 3-10, which shows the effect of various amounts of band-limiting on a 1μsec duration emission pulse. Decreasing the pass band of the receiver results in a smearing out of the sample function and gives rise to an increasingly long "tail." The degrading effect on resolution is apparent.

Finally, the effect of sample gate duration on the sample function is considered. For high resolution velocity measurements, the sample gate time must be as short as possible, consistent with other constraints. Increasing the sample

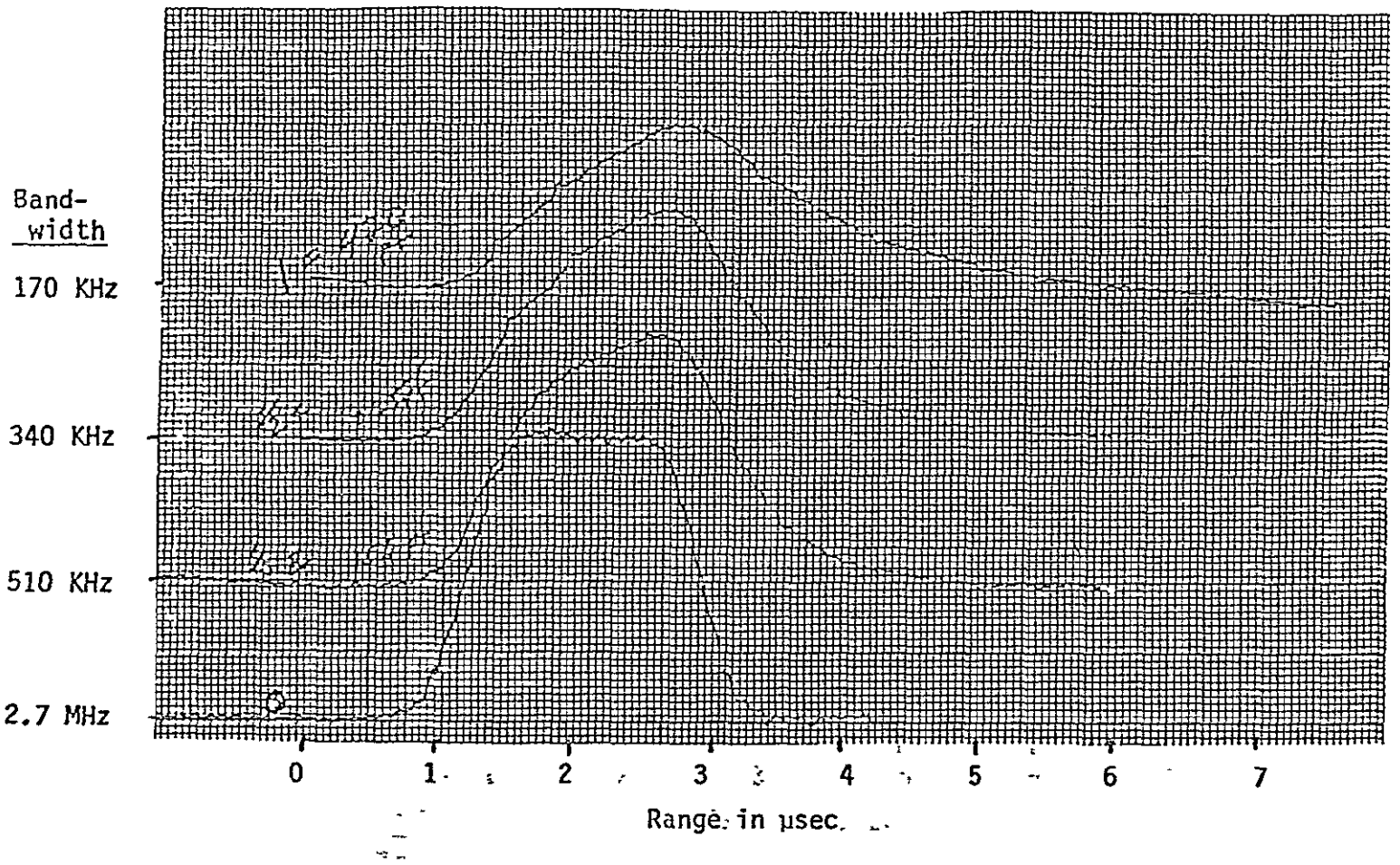

Fig. 3-10 Effect of band-limiting on sample function length.

gate time lengthens the sample function according to the relation

$$\text{sample function length} = l_o + \frac{\tau_g \cdot c}{2}$$

where l_o is the sample function length due to other factors, τ_g is the sample gate duration and c is the speed of sound.

Fig. 3-11 shows the effect of increasing sample gate times on sample function length for three separate emission pulse durations. Note that as the gate time, τ_g, increases from ¼μsec to 2μsec, resolution is significantly degraded. The reduction in peak power which occurs with the longer gate times is due to the fact that the emission power is constant, resulting in sample functions that enclose equal areas.

Figs. 3-6 through 3-11 illustrate the usefulness of the sample region testing apparatus. The experimental curves presented allow specification of optimum measurement parameters for high resolution velocity measurements. Practical considerations such as attentuation effects with increasing range and reduced signal to noise ratio often cause the experimenter to increase emission pulse duration or sample gate duration. The consequences on resolution must be known and appreciated if meaningful results are to be obtained.

A final experimental result which should be presented is the boundary error effect in velocity profile measurement which results from effective reduction of the length of the sample function at the walls of a vessel. In the physiological case, factors such as wall motion and low signal to noise ratios can obscure this effect, but in rigid tubes with constant flow the effect is more easily observed. Fig. 3-12 shows velocity profiles measured in a 10 mm diameter tube with sample functions made increasingly long by increasing the sample gate duration. These experimental results should be compared with the theoretical profiles calculated

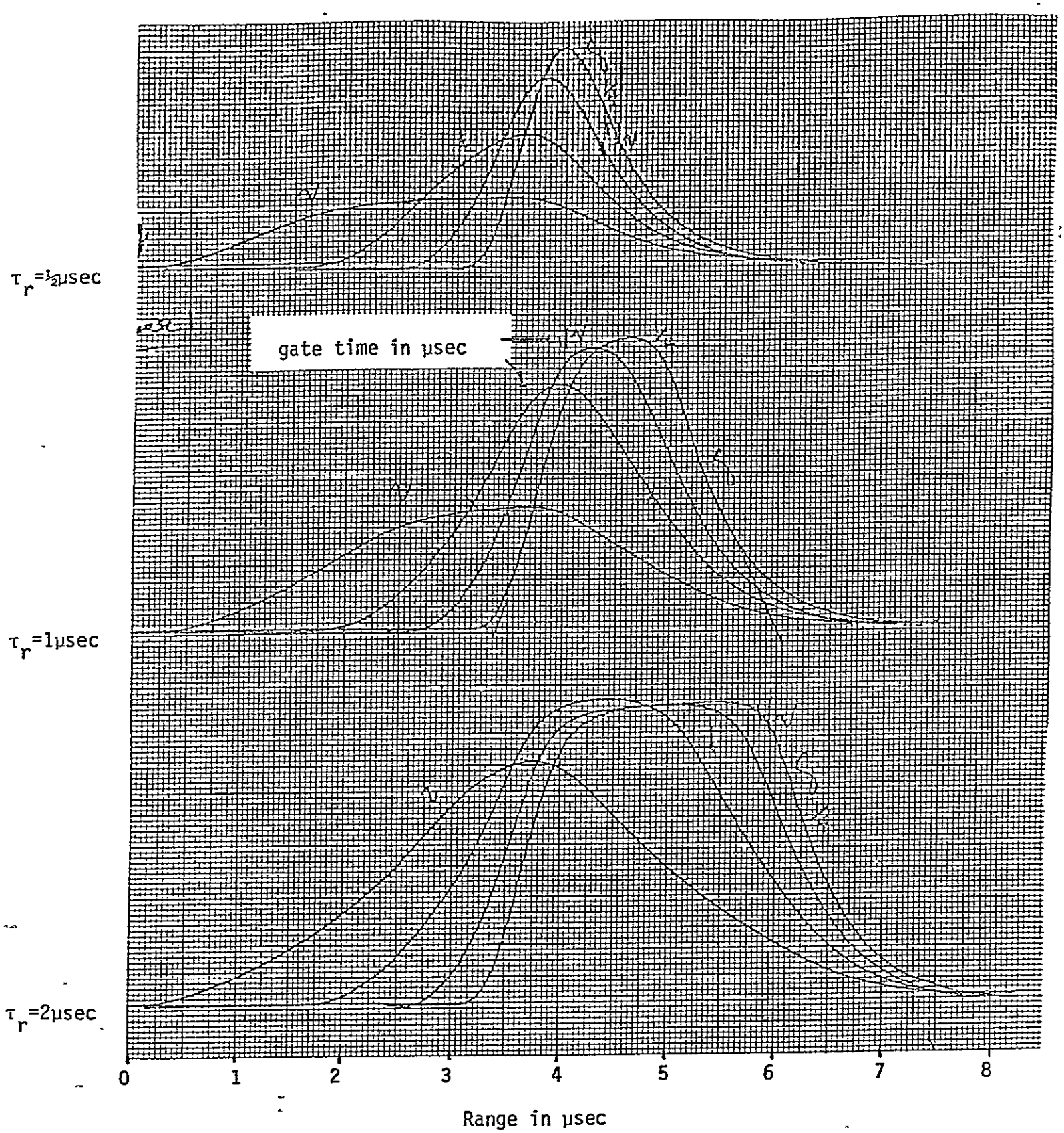

Fig. 3-11 Effect of sample gate on sample function length.

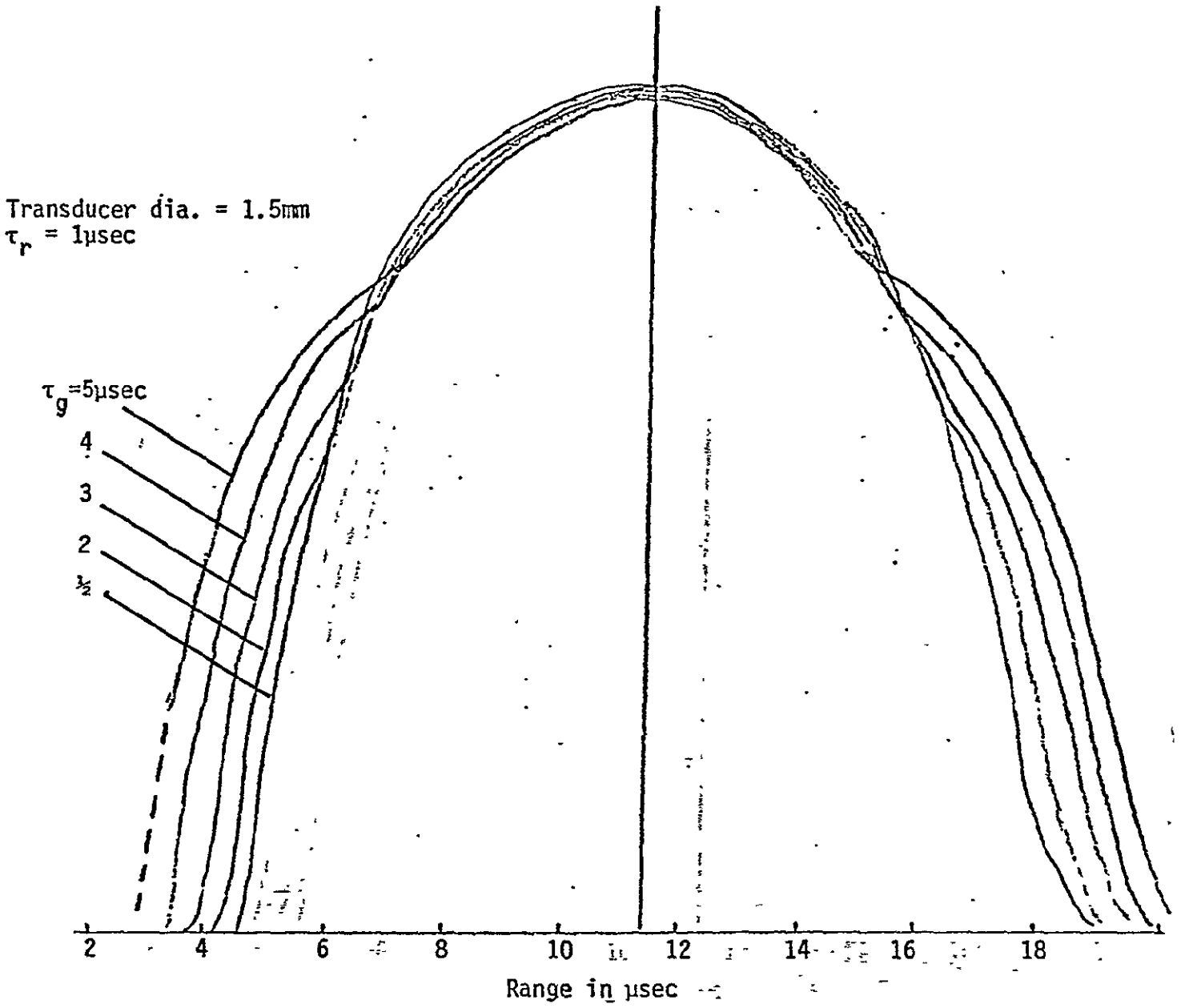

Fig. 3-12 Measured velocity profiles in 10 mm tube for various sample function lengths.

in section II-2. Specifically, refer to Fig. 2-9 which shows very similar boundary error profile shapes for increasing sample function lengths.

4. Diameter measurement by Doppler power scanning

In addition to providing a convenient method for studying the sample function and resolution of the pulsed Doppler, the step response provides an accurate and precise method of determining vessel wall locations. The location of each vessel wall is defined as the point at which the sample function is exactly centered on the wall and therefore halfway into the flowstream. With the sample function half in and half out of the flowstream, the number of scatterers and thus the returned signal power is one half that obtained when the function is totally within the flowstream. A power recording across the vessel is required to locate both walls and determine the vessel diameter. Since the location of each wall is given by the ½ power point of the power scan, the diameter is simply the ½ power width of the power curve.

Accuracy of the measurement is not resolution limited, but is limited only by one's ability to determine the ½ power point. Typically the ambiguity in finding this point is limited by four factors.

1) Ambient Noise. The quality of the power scan is affected by the Doppler signal to noise ratio (S/N). Both base line shifts and signal variance are present with poor S/N. In practice this is not a problem, however, when S/N ratios on the order of 20 to 50 dB are obtained.

2) Wall motion and wall motion "Noise." Wall motion tends to "blur" the wall location during the power scan, thus a mean diameter is obtained. While the "blurring" is reduced by multichannel operation it is not completely eliminated because of the finite integration time required to measure the signal power (Rayleigh signal statistics and fading must

be integrated out). Large amplitude low frequency echoes from the wall are another wall motion problem. These echoes tend to distort the sample function near the wall and make it appear compressed. This problem is reduced by high pass filtering to eliminate the echoes. Alternately, low pass filtering can be used to select or enhance the wall echo and provide an impulse (δ) response at the wall.

3) Range Attentuation. The Doppler signal power falls off as a function of range, tending to obscure the step function endpoint. This difficulty can be eliminated either by range gain compensation, proper transducer design, or graphical correction of the power scan record.

4) A fourth and perhaps minor limitation is vessel curvature at the wall. The step function concept was developed for a plane or nearly flat surface, however a vessel wall is a curved surface. This curvature, Δ, is easily shown to be

$$\Delta = r - \sqrt{r^2 - (\frac{a}{2})^2}$$

where a is the transducer beam diameter and r is the vessel radius. Evaluation of this for a transducer diameter of .25r leads to a curvature of less than 1%.

Combination of the above limitations leads to an experimental wall location error on the order of ¼ a sample function length and a diameter error on the order of $\frac{\sqrt{2}}{4}$ times the sample function length. In practical terms the sample function length is one the order of 1 mm, thus vessel diameter measurement is on the order of $\pm$ .4 mm. Although seemingly precise, this is still a 10% error on a 4 mm vessel. Presumably this error will be reduced as the sample function length is decreased with improved instrumentation and experience.

IV. A Proposed Method for Transcutaneous Volume Flow Measurement

1. Principles of measurement technique

One of the goals of this research has been to develop an optimal technique for the transcutaneous measurement of volume blood flow using ultrasound. By optimal is meant a technique which has the best combination of accuracy, simplicity and insensitivity to experimental errors. Another important criteria for clinical work is that the measurement be made in real time and not require numerous data transformations to obtain results.

Of the three volume flow measurement techniques, the method which claims the best combination of the above mentioned features is the uniform illumination method. This may seem surprising in view of the fact that the PUDVM, with its ability to resolve spatial velocity distributions, has been hailed as the next step in quantification of blood flow. If the desired parameter is volume blood flow, however, uniform illumination wins out.

Referring again to Table 2-1, we see that the most significant errors in applying the uniform illumination method are limited to three main sources. These are 1) errors introduced by improper Doppler angle setting; 2) errors introduced by zero-crossing detection of the Doppler shift spectrum; and 3) errors introduced by poor resolution in the vessel diameter measurement. The elimination of zero-crossing detection errors can be accomplished using the analog first moment processor discussed previously. Methods of vessel diameter measurement have also been discussed which show promise of fair accuracy. Remaining then, is the derivation of a simple technique for setting the Doppler angle and the combining of these techniques into a single measurement procedure.

A problem that immediately arises in an attempt to derive a unified technique is one of transducer size. The uniform illumination method of average

velocity determination requires a transducer width greater than the diameter of the vessel under study. Accurate diameter measurement, however, generally requires a small transducer dimension, compared with the vessel diameter. Without resorting to complex, multitransducer probes, a compromise procedure must be worked out.

A second problem also relates to the number of transducer elements. One of the goals in developing an optimal volume flow measurement technique is simplicity In terms of probe design, this implies a small unit that may be held in the hand of the clinician. Since the Doppler angle is a critical parameter in the mean velocity determination, some means of setting and maintaining a known Doppler angle must be developed. Measurement of the Doppler angle requires some sort of triangulation procedure with multiple transducers.

2. Transducer design

An attempt has been made to satisfy the requirements mentioned in the previous section with a two transducer element probe. Fig. 4-1 shows the probe design and transducer configuration. Element one consists of a narrow, rectangular transducer, 2 mm in width by 10 mm in length. Element two consists of a larger transducer, 7 mm by 10 mm. Both elements are oriented such that their sound beams intersect the probe axis at 30^{o}. When the probe is located over a subcutaneous vessel with the probe axis perpendicular to the vessel axis, the sound beams intersect the vessel at a Doppler angle of 60^{o}.

Transducer element number one of the volume flow probe is used in mean velocity determinations. It can be operated in the transmit/receive mode with the PUDVM using a wide sample gate which encompasses the cross-section of the vessel. Transducer element number two acts as a receiver of ultrasonic energy only and is used in setting of the Doppler angle and in diameter measurement.

3. Experimental method

The procedure involved in making a volume flow measurement is as follows:

1) The subcutaneous vessel should be located at two adjacent points (by palpation or otherwise) separated by a few centimeters and a line drawn on the skin indicating the vessel's course. The probe is then placed over this line such that the longitudinal axis is parallel to it.

2) Element number one of the probe is operated in the traditional manner with the PUDVM while element number two is connected to a separate receiver. The probe position is set by maximizing the reflected power received by element two. A squaring circuit such as used in the sound beam testing apparatus is suitable for this purpose and its output can be wired to a meter for observation. Maximizing the reflected power from the vessel sets angle σ = angle β in Fig. 4-1. If necessary the element number two receiver can be range-gated to eliminate undesired echoes from other surfaces.

3) The two wall echoes appear as large peaks on the power output vs. delay time curve from element two. These peaks can be found by scanning the power curve with a sample gate or by tracking the two peaks in a manner similar to arterial wall echo-tracking devices (Hokanson, 1972). The time delay between the two wall echo peaks gives the path length difference, Δr (see Fig. 4-1).

4) If refraction effects at the skin surface can be ignored, the diameter of the vessel can be found directly from Δr. Since $\sigma = \beta = \gamma = 60^{o}$, triangle abc is equilateral with its height equal to the diameter of the vessel. The height of an equilateral triangle is given by the formula

$$\text{height} = \frac{\sqrt{3}}{2} \cdot (\text{length of side})$$

Since the length of the side of the triangle is $\frac{2}{3}\Delta r$, the height or vessel

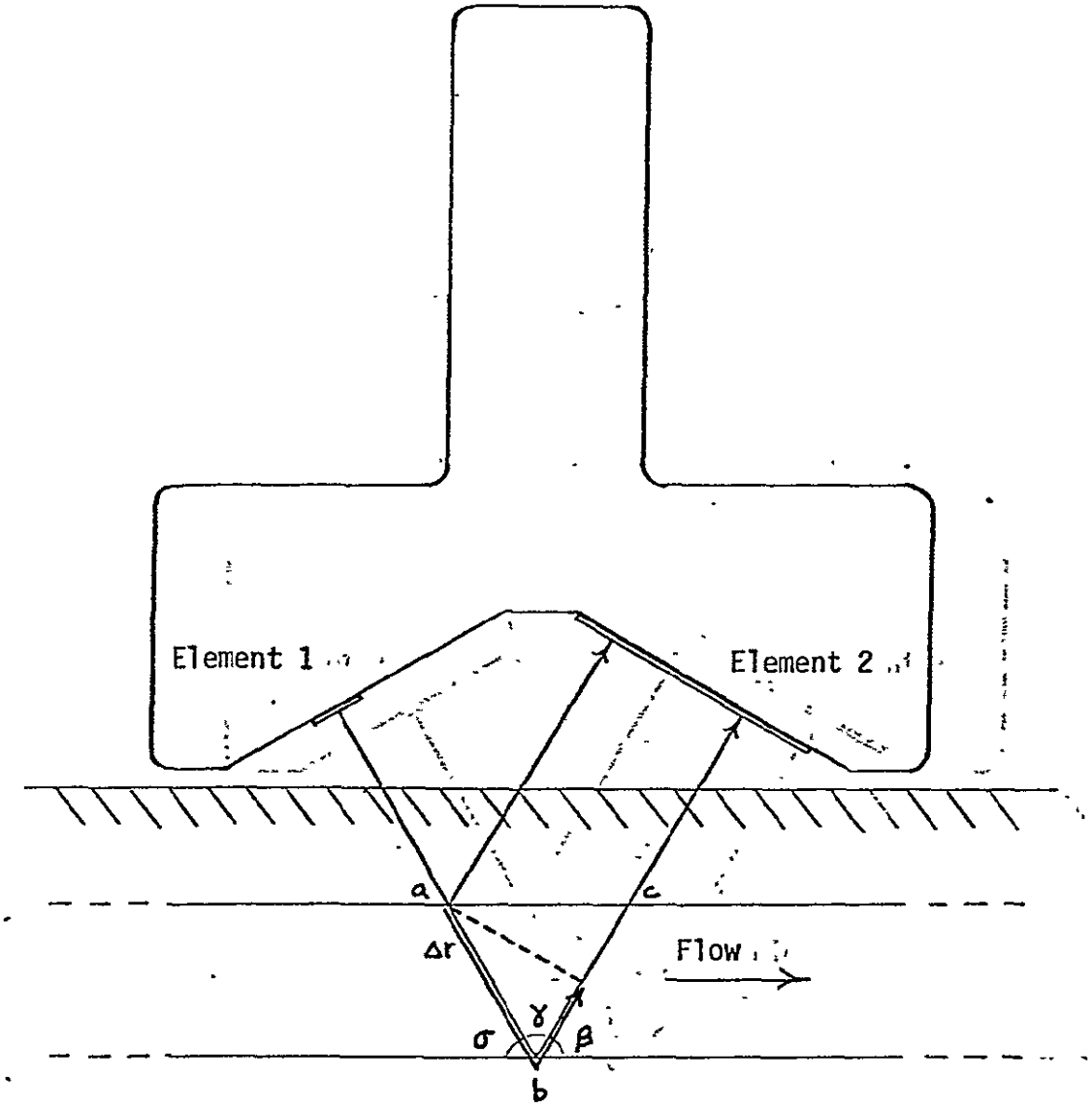

Fig. 4-1 Probe for proposed method of transcutaneous volume flow measurement.

diameter is given by

$$\text{diameter} = \frac{\sqrt{3}}{3}\,\Delta r$$

5) The average velocity over the entire vessel lumen is measured from element number one using the PUDVM with a wide sample gate. The sample gate is set to include the vessel under study but to eliminate signals from other vessels in the near vicinity. An analog first moment processor is used to process the Doppler shift signal.

This proposed method of volume flow measurement is both simple and direct. Since average velocity and vessel diameter can be computed simultaneously, these variables can be processed in a simple analog circuit to yield a voltage output directly related to volume flow. This method therefore eliminates the need for complex computer processing.

While the uniform illumination method of average velocity determination is employed in this measurement technique, it should be noted that the PUDVM is required as the measurement instrument. The vessel diameter measurement by transducer element number two requires that the ultrasound be pulsed. Range-gating of the signals from both transducers can also be employed in the typical PUDVM manner to eliminate undesirable signals.

This method of volume flow measurement is currently undergoing testing and evaluation in fluid test system trials. It is being compared with other, more traditional methods of volume flow measurement, such as timed volume collections. The accuracy of the diameter measurement technique is also being assessed. If the method survives these trials, the testing will proceed to trials on experimental animals.

V. References

Baker, D. W. (1970). Pulsed ultrasonic Doppler blood-flow sensing. IEEE Trans. on Sonics and Ultrasonics. SU-17: 170-185.

Bachman, N. M. (1966). Noise and its Effects on Communications, McGraw Hill, Inc., New York. Ch. 4.

Daigle, R. E. (1974). Aortic flow sensing using an ultrasonic esophageal probe. Ph.D. Thesis, Colorado State University.

Flax, S. W., J. G. Webster, and S. J. Updike. (1971). Statistical evaluation of the ultrasonic blood flowmeter. ISA Trans., 10(1).

Hokanson, D. E., D. J. Mozersky, D. S. Sumner, and D. E. Strandness, Jr. (1972). A phase-locked echo tracking system for recording arterial diameter changes in vivo. J. Appl. Physiol. 32: 728-733.

Jorgensen, J. E., D. N. Campau, and D. W. Baker. (1973). Physical characteristics and mathematical modelling of the pulsed ultrasonic flowmeter. Med. and Biol. Eng., pg. 404-420.

McLeod, F. D., R. E. Daigle, C. W. Miller, R. J. Morgan, and M. B. Histand. (1974). A digital Doppler velocity profile meter. In Proc. 11th Ann. Rocky Mountain Bioeng. Symp. ISA BM 74301. 61-66.

McLeod, F. D. and M. Anliker. (1971). A multiple gate pulse Doppler flowmeter. IEEE Sonics and Ultrasonics Symp., Miami Beach, p. 51.

Peronneau, P., J. Hinglais, M. Pellet, and F. Leger. (1970). Vélocitmètre sanguin par effet Doppler à émission ultrasonore pulsée. L'Onde Électrique. 50: 369-384.

Rice, S. O. (1944). Mathematical analysis of random noise, In Bell System Technical Journal, 23: 282.

Rushmer, R. F., D. W. Baker, and H. F. Stegall. (1966). Transcutaneous Doppler flow detection as a nondestructive technique. J. of Appl. Physiol. 21(2): 554-566.

Wells, P. N. T. (1969). A range-gated ultrasonic Doppler system. Med. Biol. Engr. 7: 641-652.